Available online at www.CivileJournal.org

Civil Engineering Journal

(E-ISSN: 2476-3055; ISSN: 2676-6957)

Vol. 11, No. 08, August, 2025

Statistical Optimization of Blending Conditions and Performance Evaluation of Optimal Bio-Asphalt Content

Varun Kumar T.H. [1], Muthukumar Mayakrishnan [1*], Murugavelh Somasundaram [2]

[1] School of Civil Engineering, Vellore Institute of Technology, Vellore 632014, India.

[2] CO_2 Research and Green Technologies Centre, Vellore Institute of Technology, Vellore, 632014, India.

Received 25 April 2025; Revised 17 July 2025; Accepted 21 July 2025; Published 01 August 2025

Abstract

To mitigate environmental impacts and promote sustainability in highway construction, this study investigates the optimization of blending conditions and the performance evaluation of bio-modified asphalt binder incorporating bio-asphalt derived from the pyrolysis of waste cooking oil (WCO) and low-density polyethylene (LDPE). A response surface approach was employed to optimize key blending parameters—temperature, speed, and time—based on critical physical properties of the binder. Furthermore, the optimized bio-asphalt binder was further evaluated through rheological performance tests (multiple stress creep recovery and linear amplitude sweep) and mechanical performance tests (Marshall stability, tensile strength ratio, resilient modulus, indirect tensile fatigue, and dynamic creep). The optimal conditions were identified as 130°C, 1000 rpm, and 42.37 min. Statistical validation using ANOVA, residual analysis, leverage, and Cook's distance confirmed the model's reliability, with prediction errors remaining below 5%. The bio-modified asphalt binder exhibited enhanced elastic recovery and reduced non-recoverable creep compliance (Jnr), indicating superior resistance to permanent deformation in comparison with the control asphalt binder. Additionally, the bio-modified asphalt mixture demonstrates superior Marshall stability, resilient modulus, tensile strength ratio, retained stability, and resistance to deformation in comparison with the control asphalt binder. These results demonstrate the potential of bio-asphalt as a viable, eco-friendly modifier for asphalt binders in tropical climates.

Keywords: Bio-Asphalt; Blending Parameters; Bio-Modified Asphalt Binder; Bio-Modified Asphalt Mixture.

1. Introduction

Asphalt binder, which is derived from the refining of crude oil, serves as a key binding agent in the construction of asphalt concrete for highway pavement [1]. In 2020, the global demand for asphalt binder was approximately 143 million metric tons per year (MMTPA), with a projected annual growth rate of 3.6%. By 2025, this demand is expected to rise to around 174 million metric tons annually. In major Asian markets, the demand in 2020 was about 39 MMTPA, with forecasts indicating an increase at an annual growth rate of 3.0%, reaching around 45 MMTPA by 2025 [2]. China's demand is anticipated to lead this growth, followed by India and Thailand. Despite this increasing demand, advancements in petroleum refining technology have led to a decrease in asphalt binder production. In response to these challenges, researchers and industry practitioners are actively exploring alternative binders to either partially or fully replace traditional asphalt, aiming to enhance the sustainability and environmental friendliness of asphalt products [3–5]. Bio-asphalt binders, made from biomass and biowaste materials, have gained attention due to their renewable nature, eco-friendly properties, cost-effectiveness, and lower energy consumption compared to traditional asphalt binders [6–

* Corresponding author: mmuthukumar@vit.ac.in

http://dx.doi.org/10.28991/CEJ-2025-011-08-014

8]. Bio-asphalt (BA) is typically produced by mixing bio-oil with asphalt binder or by modifying bio-oil with additives [9–11]. Raw bio-materials such as waste wood, maize stover, animal waste, castor oil, sunflower oil, and waste cooking oil are used to produce bio-oils for BA binder production [12, 13]. The use of BA binders plays a crucial role in improving pavement performance, managing waste disposal, and promoting both economic viability and environmental sustainability [12, 14–16].

Waste cooking oil (WCO) is the oil and fat used in cooking or frying, commonly found in restaurants and food service industries [17, 18]. It is a mixture of vegetable oils such as sunflower, soya, palm, and rapeseed, along with free fatty acids, monoglycerides, diglycerides, and triglycerides, which usually account for 5% to 20% of the total weight [17, 19]. These components are produced as by-products during the frying process [20]. In 2018, the WCO sector was valued at $6041.2 million and is expected to reach $8886.7 million by 2026, with a compound annual growth rate (CAGR) of 5.0% from 2019 to 2026 [21]. The USA is the largest producer, generating approximately 5.5 million tons annually, followed by China with 5 million tons, India with 3 million tons, and the European Union with 1 million tons. The remaining countries collectively produce around 2 million tons of WCO per year [18]. In general, the elemental composition of waste cooking oil (WCO) is comparable to that of asphalt binder, making it a viable additive for asphalt modification [22, 23]. Numerous studies have explored the use of WCO in asphalt binders, consistently reporting that its incorporation results in a softer binder with reduced viscosity [22, 24–27]. For instance, Portugal et al. [28] demonstrated that adding WCO to asphalt binder increases the penetration value while lowering the softening point and rutting factor, thereby enhancing the fatigue life of the binder. In another study, Saboo et al. [24] investigated the combined effect of nanoclay and WCO in asphalt binders. Their findings indicated improved rutting resistance; however, excessive nanoclay content adversely affected fatigue life. They recommended optimal dosages of 2.5% WCO and 4.6% nanoclay for better performance. Furthermore, research by Ruiken et al. [29] highlighted that a combination of WCO and crumb rubber from waste tires significantly improved rutting resistance at high temperatures and reduced cracking susceptibility at low temperatures. Additionally, Wen et al. [3] examined the use of bio-asphalt derived from WCO in hot mix asphalt. Their results showed a reduction in dynamic modulus, indicating a softer mix, along with decreased resistance to both rutting and fatigue cracking. Overall, while WCO contributes to improved workability and sustainability, its performance benefits must be carefully balanced with other modifiers to optimize the mechanical properties of asphalt mixtures.

Plastic pollution disrupts habitats and interferes with natural processes, diminishing ecosystems' ability to adapt to climate change. This has direct consequences for millions of people, affecting livelihoods, food production, and overall social well-being [30]. In 2020, global plastic production reached approximately 367 million tons, and by 2050, plastic waste is projected to exceed 12,000 million tons due to inadequate waste management practices [31]. In response to this growing concern, the incorporation of waste polyolefin plastics into asphalt binder has gained considerable attention. Numerous studies have demonstrated that using waste plastics as asphalt modifiers significantly enhances pavement performance. Key improvements include increased rutting resistance at elevated temperatures, reduced sensitivity to temperature variation, and decreased moisture susceptibility, commonly known as stripping [32–34]. For instance, Khedaywi et al. [35] evaluated the use of waste polyethylene terephthalate (PET) as a modifier at varying concentrations of 0%, 5%, 10%, and 15% by weight of the asphalt binder. Their findings revealed enhanced rutting resistance at high temperatures with increasing PET content; nevertheless, there was a decline in performance at lower temperatures. This improvement is mainly due to a rise in asphaltene content and a decline in resin content within the modified binder.

Similarly, Bensaada et al. [36] investigated the effect of recycled low-density polyethylene (LDPE) plastic waste on asphalt binders. Their study concluded that LDPE-modified binders exhibited improved rutting resistance; a 3% LDPE addition yielded the most optimal overall performance improvement. Further research by Ghani et al. [37] examined the influence of plastomers at concentrations of 0%, 2%, 4%, and 6% by binder weight. Results indicated a significant improvement in high-temperature performance, as demonstrated by a 95.27% increase in the $G^*/\sin(\delta)$ parameter, a key indicator of rutting resistance. Additionally, Singh & Gupta [38] assessed the impact of LDPE on hot-mix asphalt and reported superior mechanical properties, including increased stiffness, higher indirect tensile strength, and increased fatigue life. In another study, Abdullah et al. [39] evaluated asphalt mixtures incorporating plastic waste at 4%, 6%, 8%, and 10% by weight. Among these, the 4% mixture demonstrated the highest Marshall stability, while the 8% mixture exhibited the better tensile strength and creep modulus.

The temperature, time, and speed are the primary factors that influence the interaction between the asphalt binder and additives [40]. These factors ultimately determine the performance and compatibility of modified binders. In addition, it is important to understand that modified asphalt binders can often experience phase separation, a phenomenon that becomes more pronounced under certain storage conditions, such as storage time, gravitational influence, and high temperature [40, 41]. Optimization of the blending conditions for modified binders offers high performance, storage stability, and cost efficiency [42]. Thus, the design of an experiment (DOE) is a statistical method that enables the control of input factors in order to assess the influence on the response variables. By

controlling the input factors, the DOE can identify significant interactions that may be ignored if experimentation is performed with one factor at a time. The exploration of all potential combinations can be conducted using a full factorial approach; alternatively, only a subset of the potential combinations can be examined using a fractional factorial approach [43, 44]. This DOE concept can be accomplished by utilizing response surface methodology (RSM). RSM, a tool that integrates statistical and mathematical methods, is used for optimization of the response variable as influenced by independent variables [45]. Several research investigations have been conducted using RSM to optimize blending conditions. A study conducted by Menon et al. [41] investigated the influence of different blending conditions and petroleum sludge contents on the asphalt binder. The analysis used data from the softening point and penetration value to identify the optimal blending parameters. The most favorable blending parameters were determined to be a temperature of 149 °C, a speed of 1292 rpm, and a duration of 53 min. Similarly, using RSM and physical properties, Liu et al. [46] investigated optimal blending conditions for a binder modified with ground tire rubber and diatomite, examining temperature (160–190 °C), mixing time (30–60 min), and blending speed (3000–6000 rpm) as key variables. Based on the optimization, the optimal blending parameters were determined as follows: a temperature of 183 °C, a time of 55 min, and a speed of 5300 rpm.

Although extensive research has been conducted on eco-friendly and alternative asphalt modifiers, there is currently no documented study that investigates the use of a co-pyrolysis product derived from waste cooking oil (WCO) and low-density polyethylene (LDPE) at 350°C as a modifier for asphalt binder. In previous work, the authors explored the production of bio-asphalt through the pyrolysis of WCO and LDPE [47, 48]. Pyrolysis, a thermochemical process conducted in an inert atmosphere, facilitates the thermal degradation of long-chain organic compounds and yields solid, liquid, and gaseous products [34]. Specifically, co-pyrolysis of WCO and LDPE in a 1:1 ratio at 350°C produces bio-asphalt (BA) and bio-oil. BA is utilized in asphalt binder enhancement, whereas the liquid bio-oil finds applications in the energy sector, particularly as a substitute for automotive fuel. However, the literature lacks comprehensive studies focusing on the systematic optimization of blending parameters for incorporating this co-pyrolysis-derived BA into asphalt binder. This represents a clear research gap, particularly in terms of establishing optimal blending conditions to maximize performance benefits. Therefore, the present study addresses this gap by employing a response surface approach to optimize the blending conditions for bio-modified asphalt binder using BA derived from WCO and LDPE. The optimization process is governed by physical performance indicators as response variables, whose statistical significance is validated through analysis of variance, diagnostic plots, Cook's distance and leverage analysis, and variance inflation factor assessment. In addition, the study investigates the influence of blending parameters on these response variables using three-dimensional surface and contour plots. To further validate the optimized bio-asphalt, a comprehensive evaluation of rheological and mechanical properties is conducted through tests such as multiple stress creep recovery, linear amplitude sweep, Marshall stability, retained stability, tensile strength ratio, indirect tensile fatigue test, resilient modulus, and dynamic creep.

The subsequent parts of this paper are described as follows: Section 2 presents the materials and methods adopted for the research, including the properties of the raw materials, the preparation of bio-modified asphalt binders, the experimental design, and the test techniques used. Section 3 presents and discusses the experimental and statistical findings, covering the optimization of blending conditions, statistical analysis of the results, and the evaluation of the optimized bio-asphalt in terms of its rheological and mechanical performance. Section 4 concludes the article by summarizing the key outcomes and offering recommendations for future research directions.

2. Materials and Methods

2.1. Asphalt Binder

This study utilizes a VG 30 grade asphalt binder sourced from a single supplier to ensure the uniformity of the original binder. The VG 30 grade asphalt binder demonstrates a penetration value of 51 dmm, a softening point of 54.5 °C, a ductility greater than 100 cm, and a viscosity of 0.6 Pa. s [47].

2.2. Bio-Asphalt

Bio-asphalt was produced from waste cooking oil and low-density polyethylene in a 1:1 ratio through pyrolysis at 350°C. The physical properties of the bio-asphalt include a penetration value of 10.30 dmm, a softening point of 62.5 ^{o}C, and a viscosity of 0.94 Pa.s [47].

2.3. Aggregates

The study utilizes crushed granite aggregates obtained from the local quarry in Vellore, India. Table 1 provides an overview of the physical properties of aggregates.

Table 1. Properties of aggregates

Test	Test results	Specification [49]
Aggregate impact value (%)	18.67	Max 24%
Specific gravity of fine aggregate	2.73	-
Specific gravity of coarse aggregate	2.67	-
Combined flakiness and elongation test (%)	17.4	Max 30%
Water absorption value (%)	1.5	Max 2%

2.4. High-Speed Homogenizer

A high-speed homogenizer was specifically designed and developed to blend asphalt with various substitutes. It is constructed using high-quality stainless steel, which offers excellent resistance to corrosion. The high-speed homogenizer comprises a blending chamber equipped with a 1000-ml capacity with a heater, a temperature controller capable of reaching a maximum temperature of 350 ºC, and a spindle containing an impeller that can rotate at a maximum speed of 2500 rpm. Figure 1 shows a photographic view of the high-speed homogenizer.

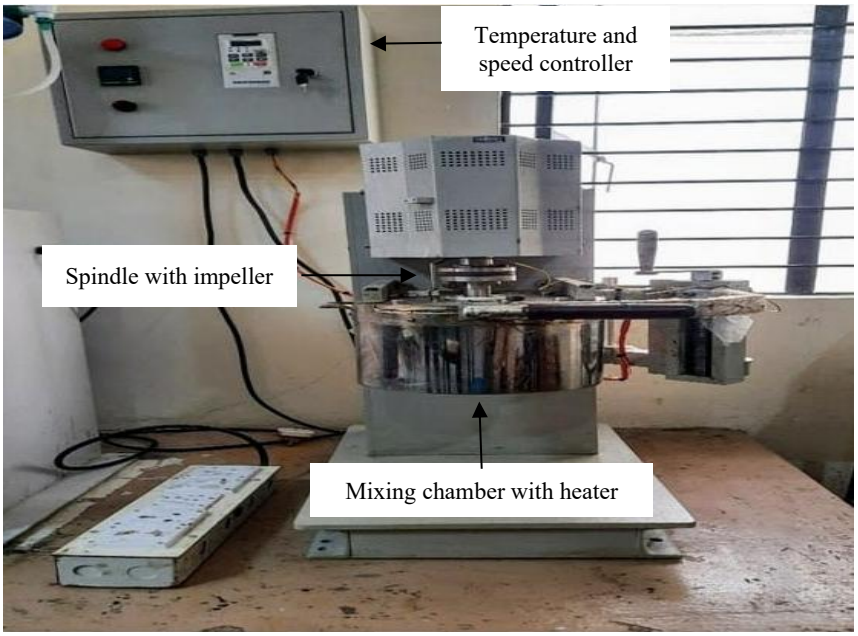

Figure 1. Photographic view of high-speed homogenizer

2.5. Preparation of Bio-Modified Asphalt Binders

The bio-modified asphalt binder was produced using a high-speed homogenizer with blending parameters that fit the RSM experimental matrix**.** After the production of the bio-modified asphalt binder using the RSM matrix, an analysis of its physical properties was performed to compare it with the standard VG30 asphalt binder according to the IS 73 guidelines [50]. A schematic of the experimental process is presented in Figure 2.

2.6. Penetration Value Test

In compliance with ASTM D5 specifications, the penetration value test was conducted. The results of this test were utilized as input parameters for RSM analysis. Furthermore, the data obtained from this experiment were utilized to assess the thermal susceptibility of the bio-modified asphalt binders.

2.7. Softening Point Test

As per ASTM D36, the ring-and-ball method was used to determine the softening temperature of the bio-modified asphalt binders. The results of this test were subsequently utilized as input parameters for RSM analysis.

2.8. Ductility Test

The ductility test was conducted on bio-modified asphalt binders to assess the adhesive nature and extensibility of bio-modified asphalt binders. This test followed the guidelines outlined in ASTM D113-17.

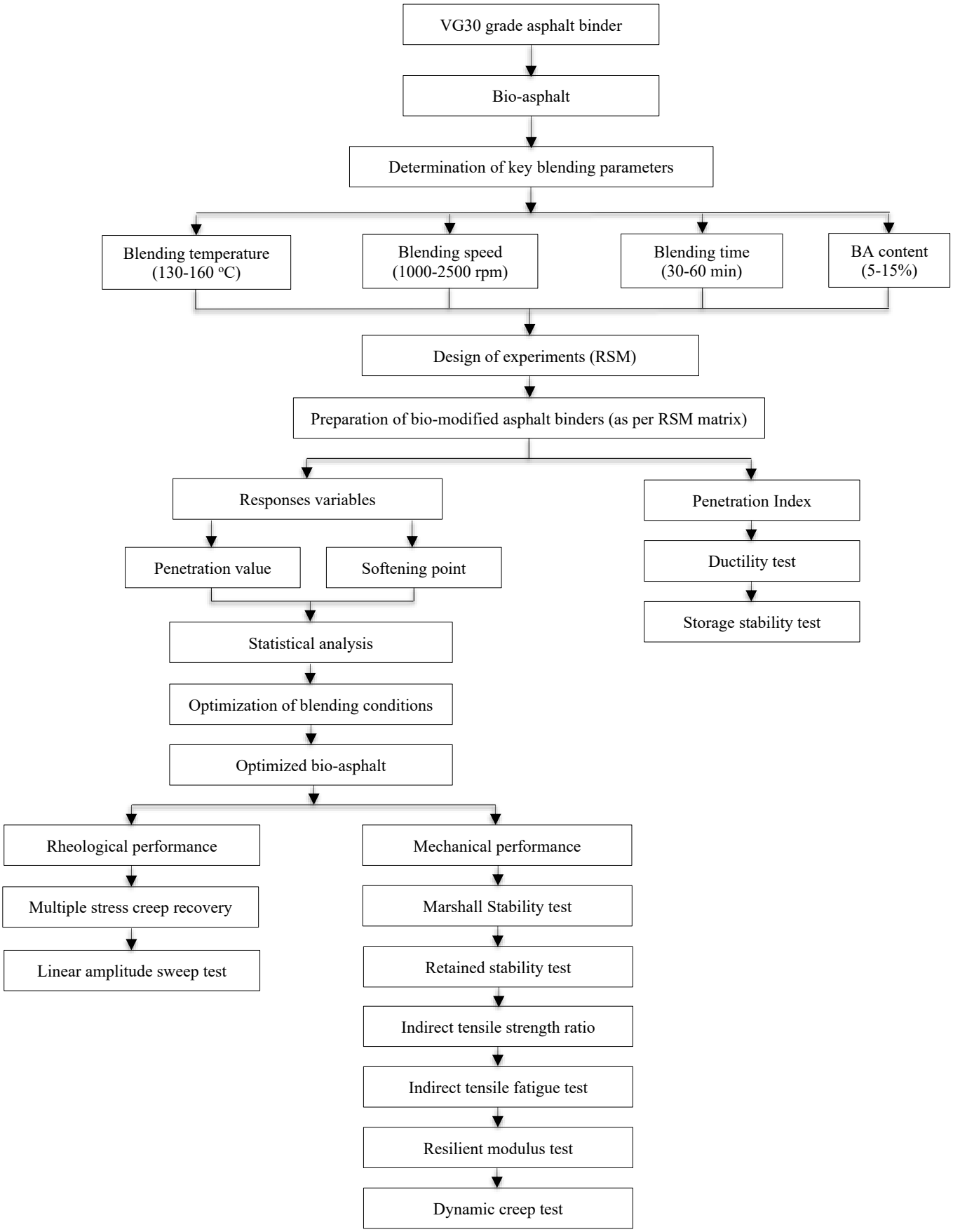

Figure 2. Schematic view of the experimental procedure

2.9. Penetration Index

The penetration index was employed to assess the temperature sensitivity of the bio-modified asphalt binders. The following Equation 1 is used to calculate the PI [51]:

$$PI = \frac{1952 - 500 \log pen - 20\,SP}{50 \log pen - SP - 120} \quad (1)$$

In this context, "pen" denotes the penetration value of bio-modified asphalt binders, while "softening point" indicates the softening point of the bio-modified asphalt binders.

2.10. Storage Stability Test

As per ASTM D5892, 50 g of bio-modified asphalt binder was introduced into a 25 mm × 140 mm aluminium cylinder and maintained vertically in an oven at 163 ± 5 °C for 48 h. It was then frozen at -6.7 ± 5°C. The aluminium tube was sectioned into three segments, and the softening points of the top and bottom portions were evaluated following ASTM D36 standard [41].

2.11. Design of Experiments Using RSM

Response Surface Methodology (RSM) is a statistical technique used to analyze problems characterized by multiple variables that influence the response. The primary objective of conducting experiments using RSM is to optimize the response [44].In this study, a face-centered central composite design was employed for the experimental design. The star points in this design, designated as α = ± 1, were located at the center of each factorial space face. Furthermore, this specific design requires three levels for each factor [44]. The Equation 2 provided is the ideal predictive model utilized to optimize the blending conditions, as given below [44]:

$$Y = \beta_o + \sum_{i=1}^{k} \beta_i X_i + \sum_{i=1}^{k} \beta_{ii} X_i^2 + \sum_i \sum_j \beta_{ij} X_i X_j + \in \quad (2)$$

where Y indicates the response, X_i X_j indicates independent variables, β_o,$\beta_{i,}$ β_{ii}, and β_{ij} are regression coefficients, and ε indicates the random error.

The study employed Design Expert software for the design of experiments. The experimental design consisted of independent variables, including the blending temperature, speed, time, and BA content. These variables were selected based on previous studies [9, 52–56]. Individual components were categorized into high and low levels. The blending temperature was set within the range of 130–160°C, and the blending speed was varied between 1000 and 2500 rpm. Similarly, the blending time was in the range of 30–60 min, and the BA content has been chosen to be between 5% and 15%, taking into account these variables. In contrast, the response variables for the bio-modified asphalt binders are penetration value and softening point. A total of 30 experimental runs have been produced using the face-centered central composite design, in which the central point is repeated six times to ensure reliability, along with fit statistics. Diagnostic plots, 3D response surface plots, leverage and Cook's distance plots, and variance inflation factors were utilized to analyze and predict the response variables. Table 2 outlines the experimental design variables and their corresponding coded values.

Table 2. Experimental Design Variables and Corresponding Coded Values

Design variables				Coded values
Blending temperature (°C)	Blending speed (rpm)	Blending time (min)	Bio-asphalt content (%)	
130	1000	30	5	-1
145	1750	45	10	0
160	2500	60	15	+1

2.12. Rheological Analysis

Rheological tests, including the multiple stress creep and recovery (MSCR) and linear amplitude sweep (LAS), were performed on the control binder as well as the asphalt binder containing the optimal bio-asphalt content.

2.12.1. Multiple Stress Creep and Recovery

Following AASHTO T350 guidelines, short-term aged binder samples were subjected to the MSCR test using a DSR (Anton Paar MCR 702 e) equipped with a 25 mm diameter spindle and a 1 mm gap. Cyclic stresses of 0.1 and 3.2 kPa (1 s creep, 9 s recovery) were applied to evaluate the elastic response of the control and bio-modified asphalt binders.

The evaluation was done at a controlled temperature of 64 °C.

2.12.2. Linear Amplitude Sweep

To evaluate fatigue life, the LAS test was carried out on long-term aged samples in accordance with AASHTO TP391 using a DSR (Anton Paar MCR 702e) fitted with an 8 mm diameter spindle and a 2 mm gap, testing both control

and bio-modified asphalt binders. The following fatigue life Equation 3 is used to compute the *A* and *B* constants for both control and bio-modified asphalt binders.

$$N_f = A\ (\gamma_{max})^B \quad (3)$$

where; $B = 2\alpha$; γ_{max} = the maximum anticipated binder strain for a specific pavement structure.

At a low strain amplitude of around 0.1%, a frequency sweep test is used to first find the undamaged material parameter α. Then, a strain sweep was conducted at a preset frequency of 10 Hz; the strain amplitude increases linearly from 0.1% to 30% over 300 s. The binder is subjected to 100 cycles at each strain level. To calculate the value of A, this data is fed into a viscoelastic continuum damage analysis. The experiment was performed at 25 ºC.

2.13. Mechanical Properties of Control and Bio-Modified Asphalt Mixtures

Mechanical properties such as Marshall stability, resilient modulus, tensile strength ratio, indirect tensile fatigue, resilient modulus, and dynamic creep tests were evaluated for the optimal bio-asphalt content (5.7%) determined by the RSM optimization technique and then compared with the control asphalt mixture.

2.13.1. Optimization of Asphalt Mixtures

The Marshall stability test is carried out to ascertain the optimal asphalt binder proportion for the control asphalt mixture as per ASTM D1559, and the mixing and compaction temperature for the control asphalt mixture and bio-modified asphalt mixture is shown in Table 3. The optimal asphalt content is determined to be 5.5% of the total mix weight, which is utilized in the preparation of the bio-modified asphalt mixture. The gradation curve for the BC mixture grade -01, as per MoRTH [49], is depicted in Figure 3. Portland cement, obtained locally with a specific gravity of 3.02, is employed as a filler material.

Table 3. Mixing and compaction temperatures for control asphalt mixture and bio-modified asphalt mixture

Type of binder	Asphalt binder	Bio-modified asphalt binder
Mixing temperature (ºC)	160	161
Compaction temperature (ºC)	156	158

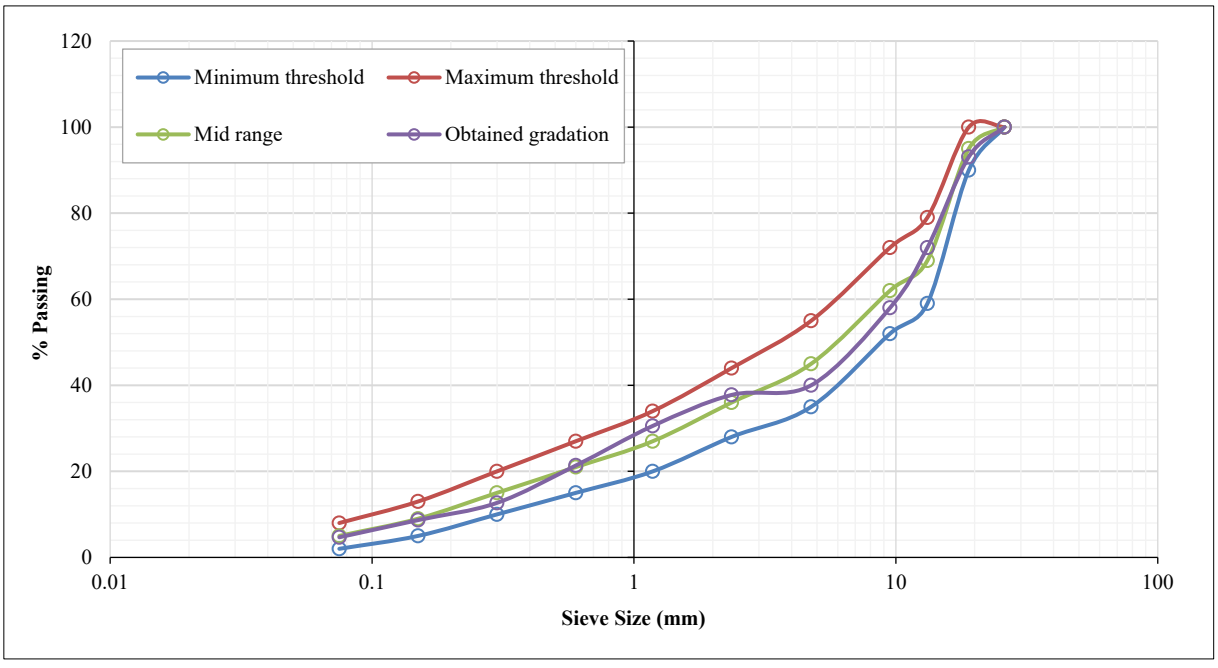

Figure 3. Gradation curve for bituminous concrete (BC) mixture

2.13.2. Retained Stability Test

Retained stability for control asphalt mixture and bio-modified asphalt mixture is conducted as per ASTM D1075.In this test, the marshal stability test is conducted on the compacted Marshall specimens before and after conditioning the specimens. The conditioned specimens are kept in a water bath at 60 °C for 24 h, and the unconditioned specimens are kept in a water bath at 60 °C for 30 min. The retained stability is assessed using Equation 4.

$$\text{Retained stability (RS)} = \frac{RS\ Conditioned}{RS\ Unconditioned} \times 100 \quad (4)$$

2.13.3. Tensile Strength Ratio Test

The tensile strength ratio (TSR) test for both the control and bio-modified asphalt mixtures was performed according to AASHTO T283 standards. TSR is defined as the ratio of the tensile strength of a moisture-conditioned specimen to that of an unconditioned one and is determined using Equation 5 [57].

$$\text{Tensile strength ratio (TSR)} = \frac{ITS\ Conditioned}{ITS\ Unconditioned} \times 100 \quad (5)$$

2.13.4. Resilient Modulus Test

The resilient modulus test for both the control and bio-modified asphalt mixtures was conducted in accordance with ASTM D4123 at temperatures of 25 °C and 35 °C. The test employed a loading frequency of 1 Hz, comprising a 0.1-s loading phase followed by a 0.9-s recovery period [58]. The applied repeated load in this test was approximately 10% of the indirect tensile strength values of both the control and bio-modified asphalt mixtures.

2.13.5. Indirect Tensile Fatigue Test

The indirect tensile fatigue test was performed at 25 °C to evaluate the fatigue life of both control and bio-modified asphalt mixtures, following the BS DD ABF (2003) guideline, using a load equivalent to 10% of the compacted Marshall specimen's indirect tensile strength.

2.13.6. Dynamic Creep Test

The dynamic creep test was conducted on both the control and bio-modified asphalt mixtures to assess permanent deformation at 60°C in accordance with EN 12697-25:2005. The samples underwent a seating pressure of 100 kPa, and tests were stopped after 3600 cycles.

3. Results and Discussion

3.1. Statistical Evaluation of Penetration Value and Softening Point Using ANOVA

Table 4 presents the experimental design matrix for the bio-modified asphalt binder. Among the trials, the maximum and minimum penetration values were recorded as 65 and 47 dmm, corresponding to run numbers 19 and 9, respectively. For the softening point, the highest value observed was 79.4°C in run number 20, while the lowest was 56.2°C in run number 11. Based on statistical analysis, the software identified a quadratic model as the best fit for both penetration and softening point values, confirmed by p-values below 0.05, indicating statistical significance. The findings from the analysis of variance (ANOVA) for penetration and softening point values, after the removal of insignificant terms, are presented in Tables 5 and 6. The model F-values for penetration and softening point were found to be 48.67 and 246.95, respectively. These high F-values suggest that the models are highly significant, with only a 0.01% probability that these results could be due to random variation. Furthermore, all p-values for the regression models are below 0.05, affirming the substantial influence of blending factors, such as temperature, speed, time, and BA content, on the response variables. Additionally, the lack-of-fit tests for both models were found to be statistically insignificant, confirming the reliability of the fitted models.

The coefficients of determination (R^2) for penetration and softening point were 0.9393 and 0.9847, respectively, both exceeding the threshold of 0.7, which indicates a significant relationship exists between the predicted and actual values. The adjusted R^2 and predicted R^2 values for both models differ by less than 0.2, suggesting close agreement and further supporting model robustness. Moreover, the adequate precision values, 31.2533 for penetration and 42.9585 for softening point, greatly exceed the recommended minimum value of 4, indicating that the models provide an adequate signal and are suitable for navigating the design space effectively [41]. As a result, the developed regression models can effectively forecast the response variables. The corresponding mathematical equations relating penetration and softening point to the independent variables are provided in Equations 6 and 7.

$$Y_1 = 55.83 - 1.06 * A - 1.28 * B - 1.06 * C - 4.06 * D + 1.75 * A * C + 1.50 * C * D - 2.22 * D^2 \quad (6)$$

$$Y_2 = 65.65 + 0.9611 * A + 0.6444 * B + 0.0833 * C + 9.96 * D - 0.6000 * B * D + 2.96 * D^2 \quad (7)$$

Table 4. Experimental design matrix for bio-modified asphalt binders

Run No.	Independent variables				Responses	
	A: Blending temperature (ºC)	B: Blending speed (rpm)	C: Blending time (min)	D: Bio-asphalt content (%)	Penetration value (dmm)	Softening point (ºC)
1	160	1000	30	5	58	59.1
2	145	1750	60	10	54	68.2
3	145	1750	45	10	56	65.1
4	145	1750	45	10	56	64.2
5	160	2500	30	5	55	59.4
6	145	1750	45	10	55	64.5
7	130	2500	60	15	48	77.5
8	130	1000	30	15	53	76.9
9	160	1000	30	15	47	79.2
10	130	1000	60	15	52	78.4
11	130	1000	60	5	56	56.2
12	130	2500	30	15	49	77.5
13	145	1750	45	5	56	58.3
14	130	2500	60	5	53	57.5
15	160	1000	60	5	57	57.1
16	160	1750	45	10	55	67.4
17	145	1750	45	10	57	66.2
18	160	1000	60	15	53	79.1
19	130	1000	30	5	65	56.7
20	160	2500	30	15	47	79.4
21	145	1750	45	10	55	63.9
22	160	2500	60	15	48	78.5
23	130	2500	30	5	63	58.6
24	145	1750	45	15	49	78.2
25	145	1750	30	10	59	66.7
26	160	2500	60	5	56	62.5
27	145	1000	45	10	56	64.1
28	130	1750	45	10	56	65.1
29	145	2500	45	10	55	67.5
30	145	1750	45	10	56	64.9

Table 5. Statistical overview of softening point

Fit summary for penetration value						
Source	**Sequential p-value**	**Lack of Fit p-value**	**Adjusted R^2**	**Predicted R^2**		
Quadratic	0.0038	0.0814	0.9114	0.7134	Suggested	
ANOVA model for penetration value						
Source	**Sum of Squares**	**df**	**Mean Square**	**F-value**	**p-value**	
Model	486.11	7	69.44	48.67	< 0.0001	significant
A-Blending Temperature	20.06	1	20.06	14.06	0.0011	
B-Blending Speed	29.39	1	29.39	20.60	0.0002	
C-Blending time	20.06	1	20.06	14.06	0.0011	
D-Bio-asphalt content	296.06	1	296.06	207.50	< 0.0001	
AC	49.00	1	49.00	34.34	< 0.0001	
CD	36.00	1	36.00	25.23	< 0.0001	
D^2	35.56	1	35.56	24.92	< 0.0001	
Lack of Fit	28.56	17	1.68	2.96	0.1168	not significant
Fit statistics for penetration value						
Std. Dev.	1.19	R^2	0.9393			
Mean	54.50	Adjusted R^2	0.9200			
C.V. %	2.19	Predicted R^2	0.8686			
		Adeq Precision	31.2533			

Table 6. Statistical overview of softening point

Fit summary for softening point						
Source	**Sequential p-value**	**Lack of Fit p-value**	**Adjusted R^2**	**Predicted R^2**		
Quadratic	0.0006	0.1205	0.9765	0.9381	Suggested	
ANOVA model for softening point						
Source	**Sum of Squares**	**df**	**Mean Square**	**F-value**	**p-value**	
Model	1868.07	6	311.35	246.95	< 0.0001	significant
A-Blending Temperature	16.63	1	16.63	13.19	0.0014	
B-Blending Speed	7.48	1	7.48	5.93	0.0231	
C-Blending time	0.1250	1	0.1250	0.0991	0.7557	
D-Bio-asphalt content	1786.03	1	1786.03	1416.61	< 0.0001	
BD	5.76	1	5.76	4.57	0.0434	
D^2	52.06	1	52.06	41.29	< 0.0001	
Lack of Fit	25.68	18	1.43	2.15	0.2031	not significant
Fit statistics for softening point						
Std. Dev.	1.12	R^2	0.9847			
Mean	67.26	Adjusted R^2	0.9807			
C.V. %	1.67	Predicted R^2	0.9746			
		Adeq Precision	42.9585			

3.2. Diagnostic Visualization of Penetration Value and Softening Point

Diagnostic plots serve as effective visual tools to assess the validity of the statistical model, the accuracy of the dataset, and the normality of the residual distribution. Figures 4-a and 5-a display the normal probability plots of residuals for penetration value and softening point, respectively. In both cases, the residual points lie closely along a straight line, indicating that the residuals are normally distributed. Figures 4-b and 5-b illustrate the plots of residuals versus predicted values for the two responses. The random and scattered distribution of residuals along the zero-reference line suggests the absence of systematic error, confirming that the model provides a good fit for the data. Additionally, the histogram plots shown in Figures 4-c and 5-c further support the normality of residuals. The symmetrical shape and lack of extreme values in these plots indicate the absence of outliers for both penetration value and softening point. Figures 4-d and 5-d present the residuals versus run order plots. The residuals appear sinusoidally scattered above and below the central line, suggesting no apparent pattern and affirming the model's predictive reliability and consistency throughout the experimental sequence. Moreover, Figures 4-e and 5-e depict the predicted versus actual values for both response variables. The residuals points lie close to the 45-degree line, demonstrating a close alignment between the predicted and actual values and thus confirming the model's predictive accuracy. Eventually, Figures 4-f and 5-f illustrate the perturbation plots for penetration value and softening point. The sloping and curvilinear trends observed in these plots reflect the sensitivity of the responses to changes in the input variables, thereby emphasizing the significant influence of process conditions on the performance outcomes.

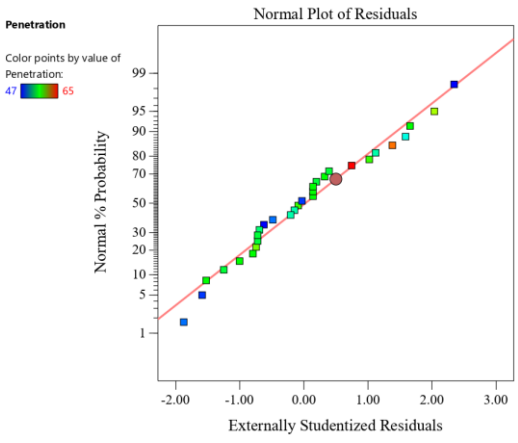

(a)

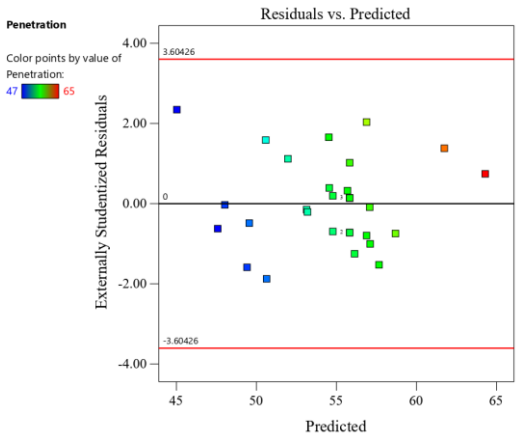

(b)

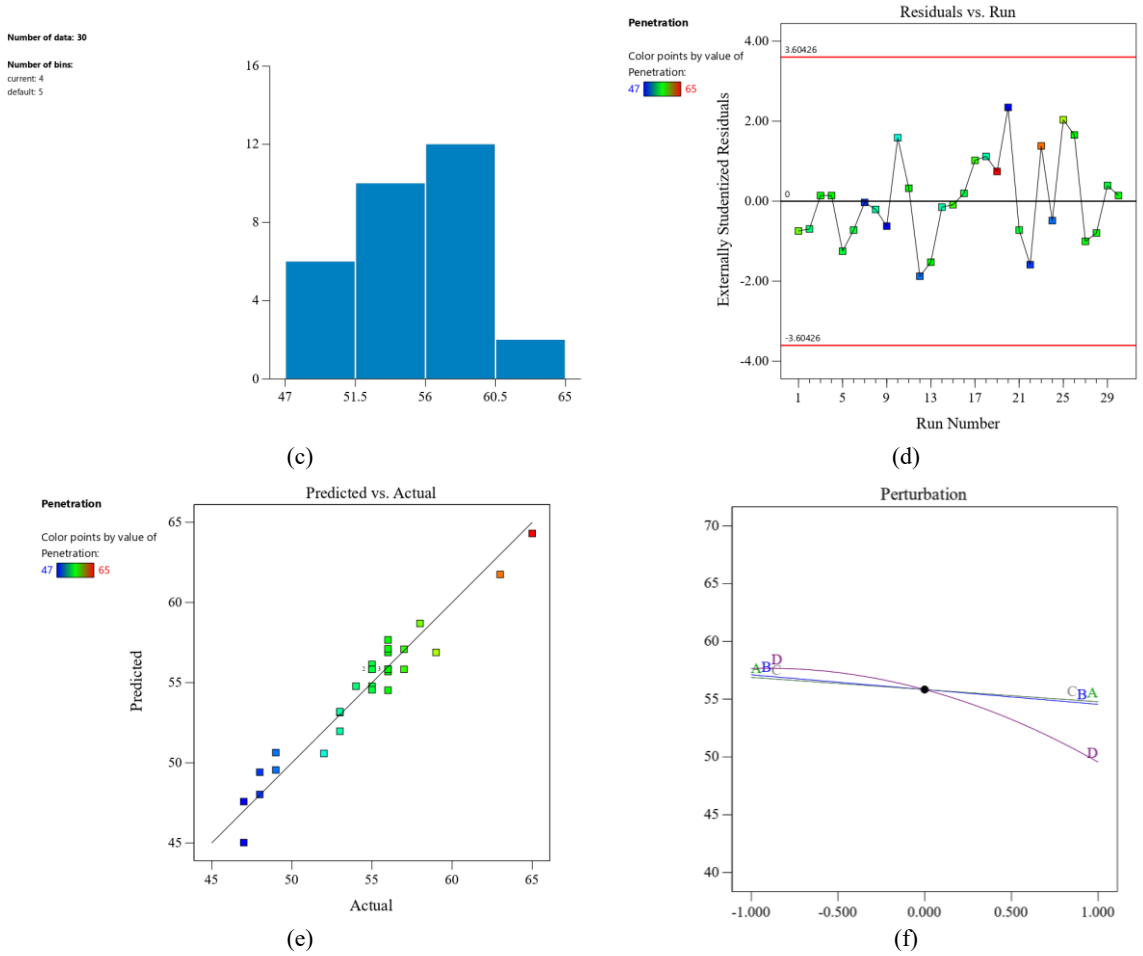

Figure 4. Diagnostic plots for penetration value

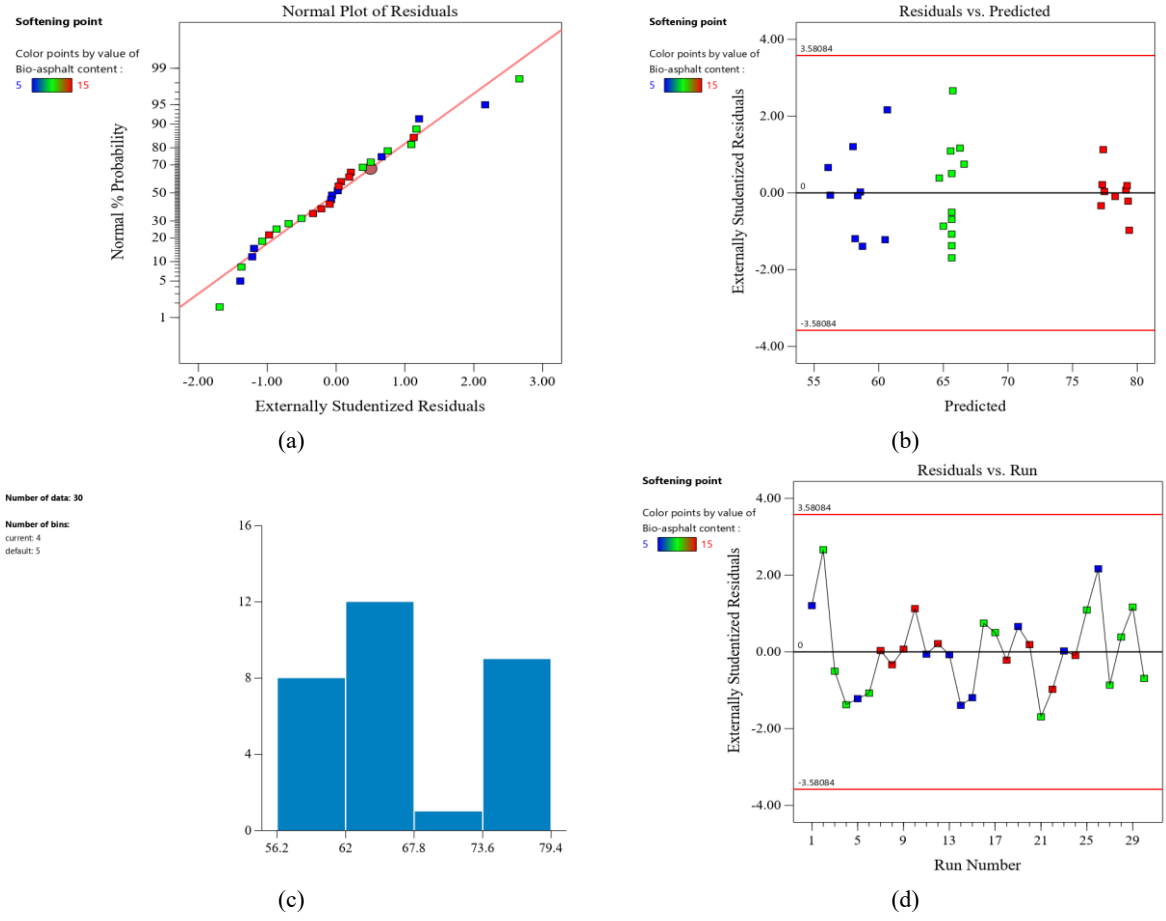

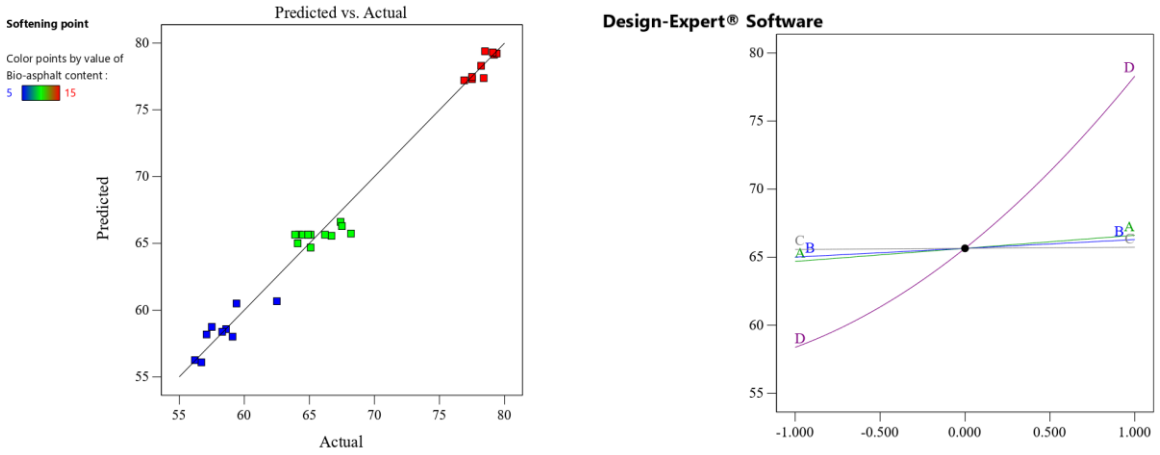

Figure 5. Diagnostic plots for softening point

3.3. Effects of Blending Conditions on Penetration Value and Softening Point: 3D Response Surface and Contour Plots

The penetration value of the asphalt binder is significantly influenced by blending temperature, blending time, blending speed, and BA content, as confirmed by statistical analysis with p-values less than 0.005. Among these factors, BA content exerts the most pronounced effect, as indicated by a highly significant p-value below 0.0001, as presented in Table 5. The influence of these variables is further illustrated in the 3D response surface and contour plots presented in Figures 6-a to 6-f, which depict the interactive effects between penetration value and each of the blending parameters, including BA content, temperature, speed, and time. As observed from the plots, the penetration value consistently decreases with increasing BA content, blending temperature, blending speed, and blending time. This decreasing trend is primarily attributed to the modifications in the physiochemical properties of the asphalt binder resulting from its interaction with BA. Bio-asphalt contains several aliphatic, non-polar compounds such as pentadecane, heptadecene, and dodecane [47] that contribute to these changes. The observed reduction in penetration value is beneficial, as it indicates enhanced resistance to rutting of the modified binder, enhancing its performance under high-temperature conditions [30].

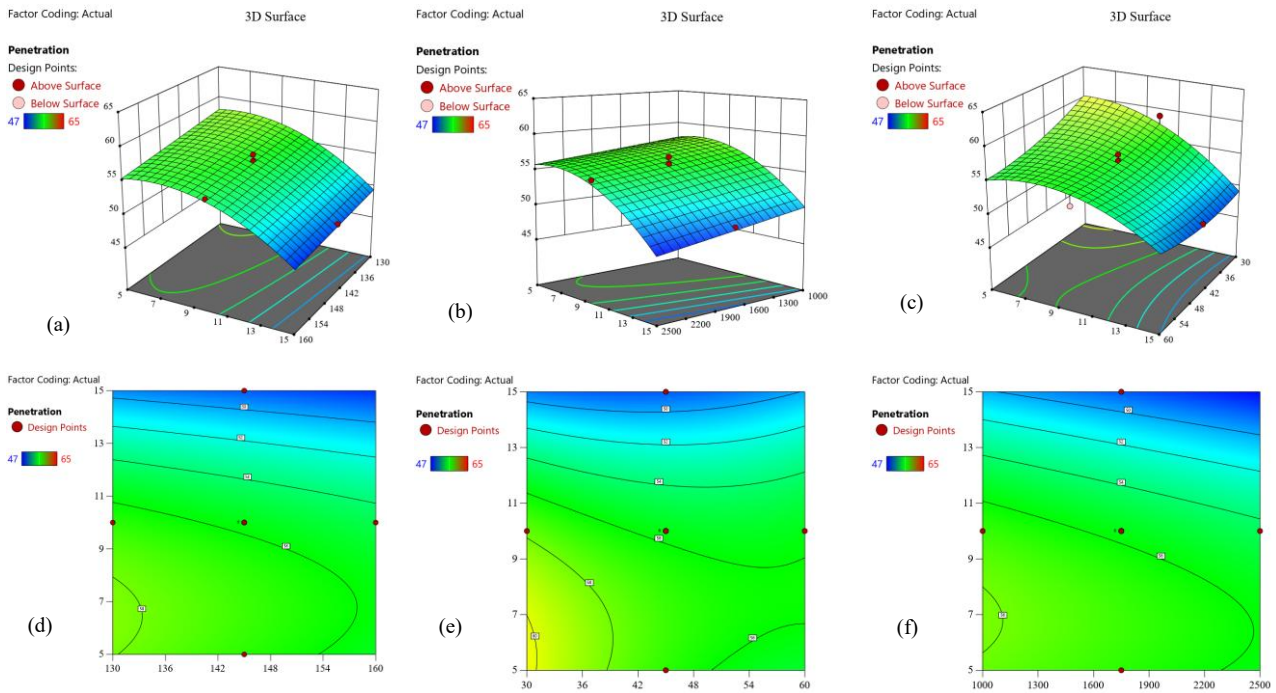

Figure 6. 3D response surface and contour plots for penetration value

Figure 7 presents the 3D graphical response surfaces and contour plots representing the variation in softening point with respect to BA content, blending temperature, blending speed, and blending time. Specifically, Figures 7-a to 7-f depict how the softening point responds to changes in each of these parameters. The plots clearly demonstrate that the softening point increases progressively with increasing BA content, blending temperature, blending speed, and blending

time. The statistical analysis of variance confirms that these effects are significant, with p-values less than 0.05, emphasizing the importance of optimizing blending conditions. Notably, among all the variables, BA content has the most substantial influence on the softening point, as evidenced by a highly significant P-value < 0.0001 (Table 6), surpassing the influence of temperature, speed, and time. This pronounced effect is primarily ascribed to the improved interaction between the BA and the asphalt binder, which promotes an increase in the asphaltene-to-maltene ratio. Such a shift in the binder's microstructure contributes to improved stiffness and a higher softening point, thereby enhancing the binder's resistance to deformation under elevated temperature [59].

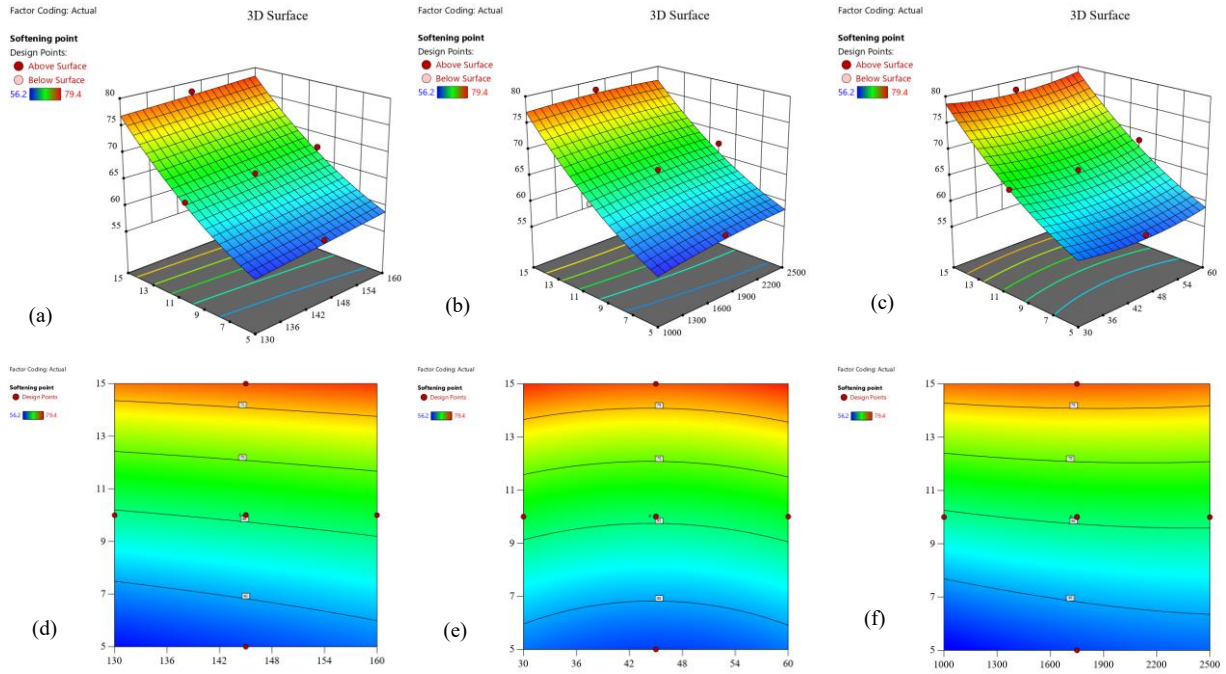

Figure 7. 3D response surface and contour plots for softening point

3.4. Leverage and Cook's Distance Value for Penetration Value and Softening Point

Table 7 presents the leverage and Cook's distance values associated with the penetration value and softening point, while Figure 8 provides a corresponding graphical representation of these diagnostic metrics. Leverage serves as an important statistical diagnostic tool that quantifies the influence of individual data points on the model's overall fit [45]. The average leverage for both penetration value and softening point is calculated based on the ratio of the number of model parameters to the total number of experimental runs. Accordingly, twice the average leverage is determined to be 0.6 for the penetration value and 0.5 for the softening point. In statistical modeling, data points with leverage values exceeding twice the average leverage are typically considered to exert an unusually high influence on the regression outcome. However, in this study, all experimental runs exhibit leverage values below these thresholds, less than 0.6 for penetration and less than 0.5 for the softening point, as detailed in Table 7. Furthermore, Figures 8-a and 8-c visually confirm that the leverage values for penetration and softening point, recorded at 0.53 and 0.46, respectively, lie well within the red reference boundary, indicating no excessive influence by any single data point.

Table 7. Leverage and cook's distance value for penetration value and softening point

Run Order	Leverage (penetration value)	Cook's distance (penetration value)	Leverage (softening point)	Cook's distance (softening point)
1	0.403	0.048	0.34	0.105
2	0.139	0.01	0.139	0.129
3	0.083	0	0.083	0.003
4	0.083	0	0.083	0.024
5	0.403	0.128	0.34	0.107
6	0.083	0.006	0.083	0.015
7	0.403	0	0.34	0
8	0.403	0.004	0.34	0.009
9	0.403	0.034	0.34	0
10	0.403	0.199	0.34	0.093
11	0.403	0.009	0.34	0

12	0.403	0.266	0.34	0.004
13	0.111	0.034	0.111	0
14	0.403	0.002	0.34	0.137
15	0.403	0.001	0.34	0.103
16	0.139	0.001	0.139	0.013
17	0.083	0.012	0.083	0.003
18	0.403	0.105	0.34	0.004
19	0.403	0.048	0.34	0.033
20	0.403	0.385	0.34	0.003
21	0.083	0.006	0.083	0.034
22	0.403	0.199	0.34	0.07
23	0.403	0.155	0.34	0
24	0.111	0.004	0.111	0
25	0.139	0.073	0.139	0.027
26	0.403	0.214	0.34	0.298
27	0.139	0.02	0.139	0.017
28	0.139	0.013	0.139	0.004
29	0.139	0.003	0.139	0.031
30	0.083	0	0.083	0.006

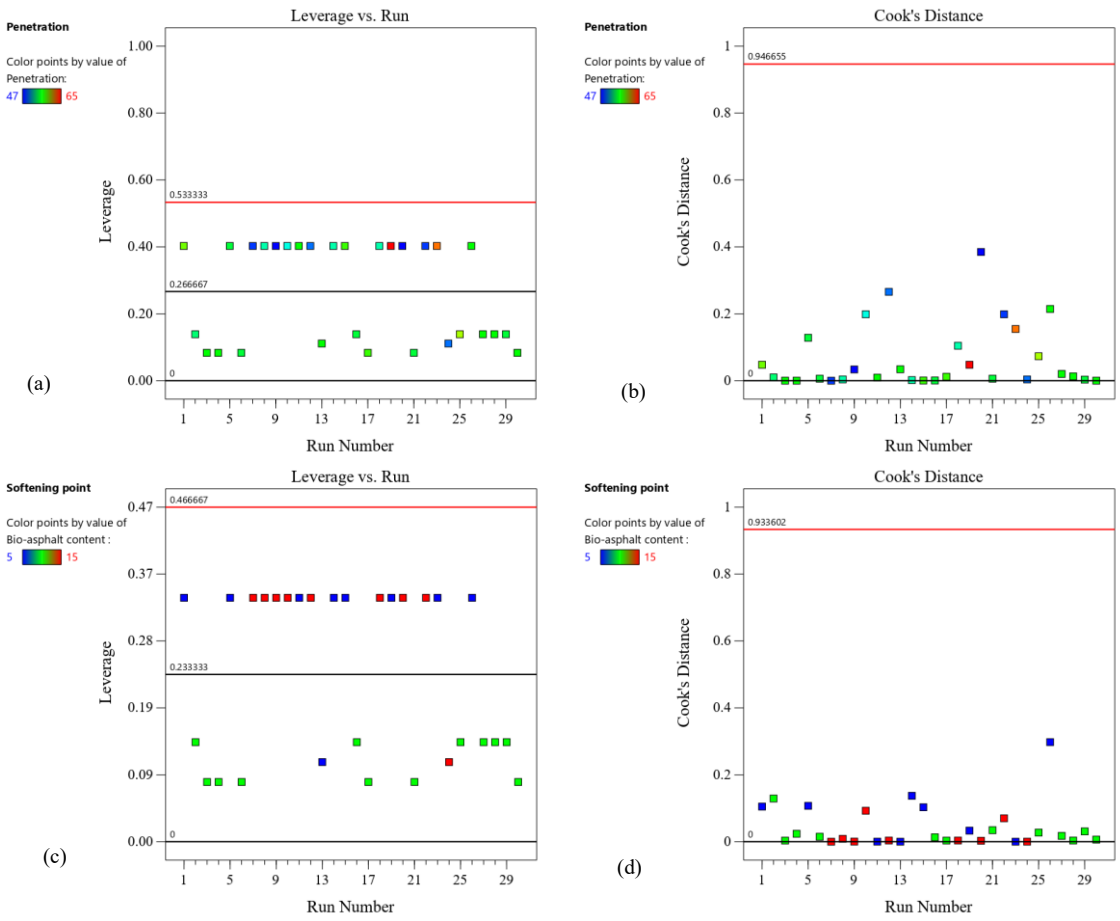

Figure 8. Leverage and cook's distance plots for penetration value and softening point

In addition to leverage, Cook's distance is employed as another diagnostic metric to assess the overall impact of each observation on the fitted regression model [45]. As shown in Table 7, the Cook's distance values for all experimental runs, both for penetration and softening point, remain below the critical threshold of 1. Specifically, Figures 8-b and 8-d reveal that the maximum Cook's distance values for penetration and softening point are 0.95 and 0.93, respectively, further confirming that none of the data points significantly distort the model. These diagnostic outcomes indicate that the developed predictive model is statistically sound, robust, and reliable.

3.5. Variance Inflation Factor for Penetration Value and Softening Point

The variance inflation factor (VIF) values for the penetration and softening point models are presented in Table 8. The variance inflation factor (VIF) evaluates the increase in the variance across the coefficient of estimate due to non-orthogonality in the design [60]. Specifically, it assesses the extent to which the non-orthogonality of the experimental design contributes to the instability or redundancy in the estimated coefficients. In general, a VIF value of 1 indicates perfect orthogonality, meaning there is no correlation among the predictor variables. Conversely, a value of VIF greater than 10 often denotes significant multicollinearity, which can hinder the effectiveness and interpretability of the regression model. In this study, the VIF values for all predictor variables, including blending temperature, blending speed, blending time, BA content, interaction terms, and polynomial terms, are equal to 1 for both the penetration and softening point models, as indicated in Table 8. This uniformity in VIF values clearly demonstrates the absence of multicollinearity among the model inputs. As a result, the design can be classified as orthogonal, signifying that the predictors are statistically independent of one another. This independence enhances the robustness and precision of the regression estimates, thereby contributing to the overall reliability and predictive strength of the developed models.

Table 8. Variance inflation factor for penetration value and softening point

Variance inflation factor for penetration value						
Factor	**Coefficient Estimate**	**Df**	**Standard Error**	**95% CI Low**	**95% CI High**	**VIF**
Intercept	55.83	1	0.3448	55.12	56.55	
A-Blending Temperature	-1.06	1	0.2815	-1.64	-0.4717	1.0000
B-Blending Speed	-1.28	1	0.2815	-1.86	-0.6939	1.0000
C-Blending time	-1.06	1	0.2815	-1.64	-0.4717	1.0000
D-Bio-asphalt content	-4.06	1	0.2815	-4.64	-3.47	1.0000
AC	1.75	1	0.2986	1.13	2.37	1.0000
CD	1.50	1	0.2986	0.8807	2.12	1.0000
D^2	-2.22	1	0.4452	-3.15	-1.30	1.0000
Variance inflation factor for softening point						
Factor	**Coefficient Estimate**	**Df**	**Standard Error**	**95% CI Low**	**95% CI High**	**VIF**
Intercept	65.65	1	0.3241	64.98	66.32	
A-Blending Temperature	0.9611	1	0.2647	0.4136	1.51	1.0000
B-Blending Speed	0.6444	1	0.2647	0.0970	1.19	1.0000
C-Blending time	0.0833	1	0.2647	-0.4641	0.6308	1.0000
D-Bio-asphalt content	9.96	1	0.2647	9.41	10.51	1.0000
BD	-0.6000	1	0.2807	-1.18	-0.0193	1.0000
D^2	2.69	1	0.4185	1.82	3.55	1.0000

3.6. Storage Stability of Bio-Modified Asphalt Binders

Figure 9 shows the storage stability values of the bio-modified asphalt binders. The modified binders were subjected to thermal and freezing conditions in an aluminium tube, after which the softening point of the modified binders was determined. If the differences between the softening point value of the upper and lower portions are below 2.2 ºC, it suggests that the binder with varying amounts of BA is evenly mixed [41]. Hence, the bio-modified asphalt binders exhibited no phase separation under different blending conditions.

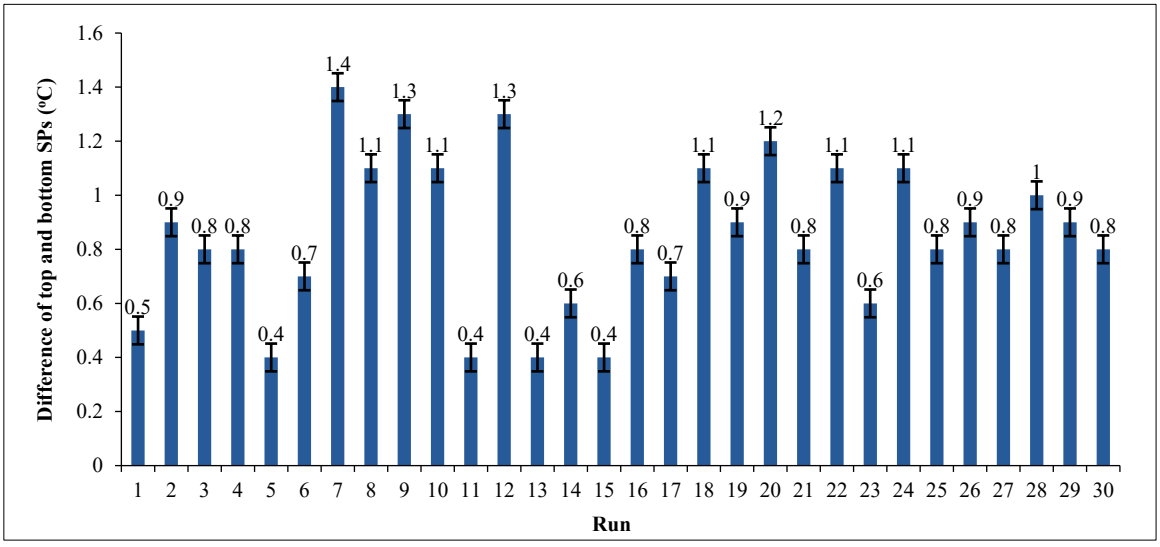

Figure 9. Strorage stability of bio-modifed asphalt binders

3.7. Ductility Value of Bio-Modified Asphalt Binders

The ductility values of the bio-modified asphalt binders are presented in Figure 10, providing a clear indication of how the incorporation of BA influences the binder's flexibility and performance at low temperatures. As illustrated in Figure 10, a noticeable decrease in ductility is observed across varying BA proportions and blending conditions. This decline becomes particularly significant when BA is incorporated at 15% by weight of the asphalt binder. At this concentration, the modified binder exhibits reduced ability to form a continuous, ductile film around aggregate particles, which is essential for maintaining flexibility and crack resistance under low-temperature conditions. As a result, the ductility values in several experimental runs fall below the minimum acceptable threshold of 40 cm, as stipulated in the IS73:2013 [50]. Specifically, this inadequacy is observed in run numbers 7, 8, 9, 10, 18, 20, 22, and 24, where the high BA content and certain blending conditions contribute to excessive binder stiffness. These findings highlight the importance of optimizing BA content and blending parameters to ensure that the modified binder retains adequate ductility and remains compliant with performance standards for cold climate applications.

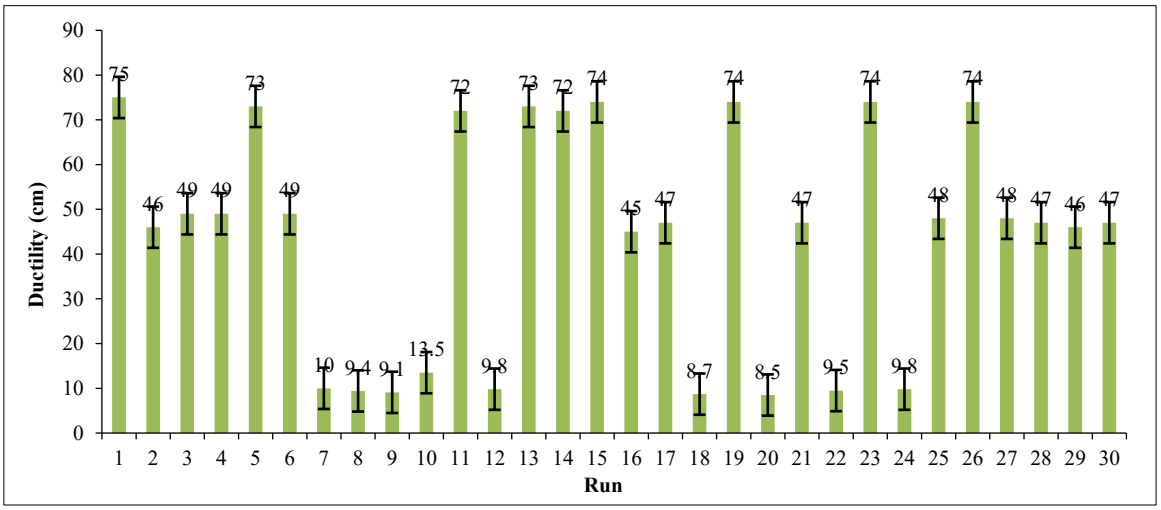

Figure 10. Ductility value of bio-modifed asphalt binders

3.8. Penetration Index of Bio-Modified Asphalt Binders

Figure 11 illustrates the Penetration Index (PI) values of the bio-modified asphalt binders under various blending conditions. As depicted in Figure 10, all PI values fall within the standard acceptable range of -3 to +7, which is commonly used to assess the thermal susceptibility of asphalt binders [61]. Typically, PI values near -3 indicate that the binder is highly susceptible to deformation at elevated temperatures, while values approaching +7 reflect increased stiffness and improved resistance to deformation at lower temperatures. These values serve as indicators of the binder's temperature sensitivity, which is critical for determining its suitability across different climatic conditions. Importantly, for regions with warm or hot climates, PI values greater than +4 are generally preferred, as they indicate enhanced resistance to rutting and better performance under high-temperature exposure. In contrast, PI values below +4 are more appropriate for moderate climates. Based on the data presented in Figure 11, it is evident that incorporating 15% BA by weight into the asphalt binder significantly influences the performance of modified binders, producing PI values exceeding +4 in run numbers 7, 8, 9, 10, 18, 20, 22, and 24. This trend highlights the potential of higher BA content to enhance the binder's high-temperature performance, particularly in warm climate conditions.

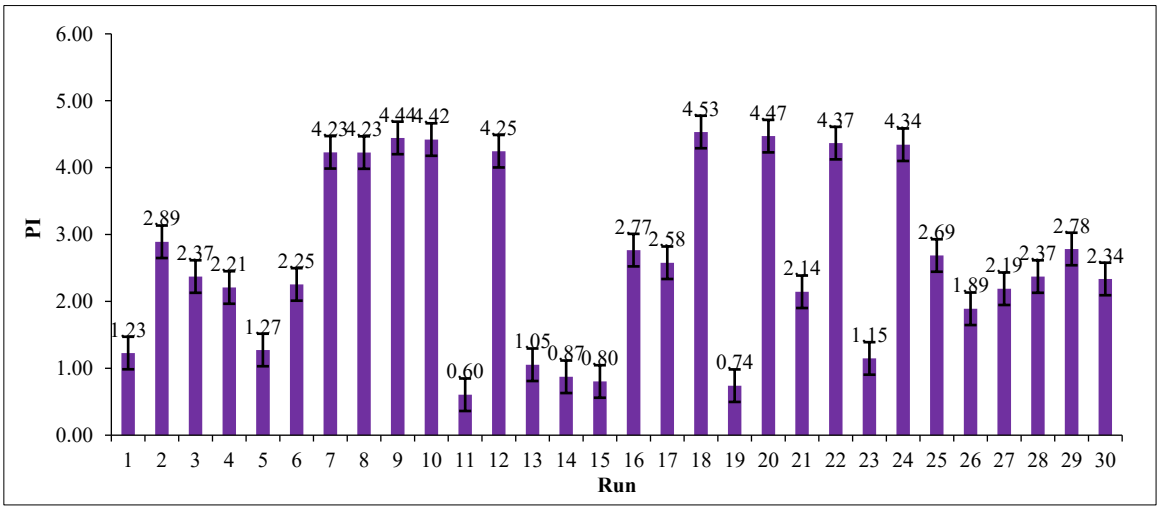

Figure 11. Penetration index of bio-modifed asphalt binders

3.9. Multi-Objective Optimization

In the present study, a multi-objective optimization technique was utilized, employing RSM to analyze the variables and determine the optimal solution [44]. The criteria that must be examined to optimize the blending conditions are critical factors that influence the efficiency of the blending process in the construction of flexible pavements [62]. To achieve optimization, the blending temperature, blending speed, and blending time were selected as their minimum values, whereas the BA content was selected as its maximum value. The specified upper and lower limits for the blending parameters were as follows: blending temperature ranged from 130 to 160 °C, blending speed was set between 1000 and 2500 rpm, and blending time was set at 30 to 60 min. The BA content was set between 5 and 15%. Furthermore, the penetration value was chosen in the range of 45 to 60 dmm, whereas the softening point was chosen in the range of 47 to 56 °C as per the IS 73 specification [47, 50]. The objective of optimization is to minimize the values of blending variables, such as temperature, speed, and time, to decrease greenhouse gas emissions and energy usage during the blending process in the asphalt industry [54]. Furthermore, the BA content was optimized to maximize its utilization of BA content in the asphalt binder, thereby promoting the development of a more sustainable asphalt binder. A graphical ramp view of the optimized blending conditions is shown in Figure 12. The responses and independent variables for the optimized value are represented by a blue and red pointer, respectively, as shown in Figure 12. The combined desirability value for the independent variable and response variable is found to be 0.678 (Figure 12), which is in the range of 0.6 to 0.8, and hence it is desirable. Furthermore, the experimental validation of the optimized value was performed three times, and the mean value was used to calculate the percentage of error (P.E). The percentage error can be calculated using Equation 8:

$$\text{Percentage Error (\%)} = \frac{|\text{Experimental value} - \text{Predicted value}|}{|\text{Experimental value}|} \times 100 \quad (8)$$

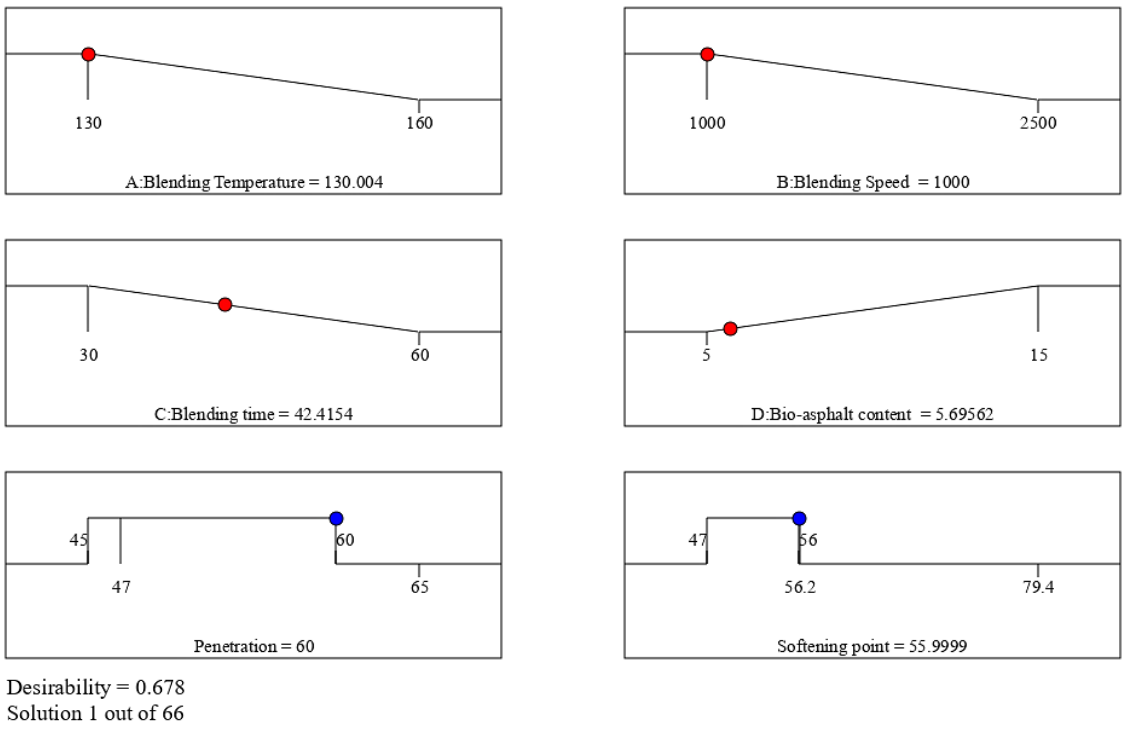

Figure 12. Graphical ramp views for optimized blending conditions

Validation of the optimized blending conditions is presented in Table 9. It has been found that the percentage error of each response was below 5%. Therefore, a strong correlation exists between the experimental and predicted outcomes when the blending conditions are optimal. Based on the optimization technique, the values for the temperature, speed, and time were determined to be 130 °C, 1000 rpm, and 42.37 min, respectively. Furthermore, the BA content is determined to be 5.7%. The aforementioned blending variables are appropriate for the preparation of a bio-modified asphalt binder.

Table 9. Validation of optimized blending conditions

Responses	Predicted value	Experimental value	Remarks
Penetration value (dmm)	60	58	P.E (%) = 3.45
Softening point (°C)	56	54	P.E (%) = 3.7

3.10. Rheological Analysis for Control Asphalt Binder and Bio-Modified Asphalt Binder

3.10.1. Multiple Stress Creep and Recovery

The MSCR test evaluates the elastic response characteristics of both control and bio-modified asphalt binders by measuring their behavior during the creep and recovery phases. This assessment is conducted at two specified stress levels, 0.1 kPa and 3.2 kPa, under a testing temperature of 64°C. In Figure 13-a, the percentage recovery for the control binder is relatively low, showing 0.93% at 0.1 kPa and decreasing to 0% at 3.2 kPa. In contrast, the bio-modified binder shows significantly higher recovery values of 2.75% at 0.1 kPa and 0.48% at 3.2 kPa, indicating enhanced elastic response under stress. Figure 13-b further supports this observation, presenting non-recoverable creep compliance (J_{nr}) values of 5.26 and 5.83 (1/kPa) for the control binder at 0.1 and 3.2 kPa, respectively, while the bio-modified binder exhibits lower values of 2.70 and 3.53 (1/kPa) at the same stress levels. These results highlight the improved elasticity and reduced permanent deformation of the bio-modified asphalt binder, especially under elevated temperatures, thereby demonstrating better performance against rutting than the control asphalt binder.

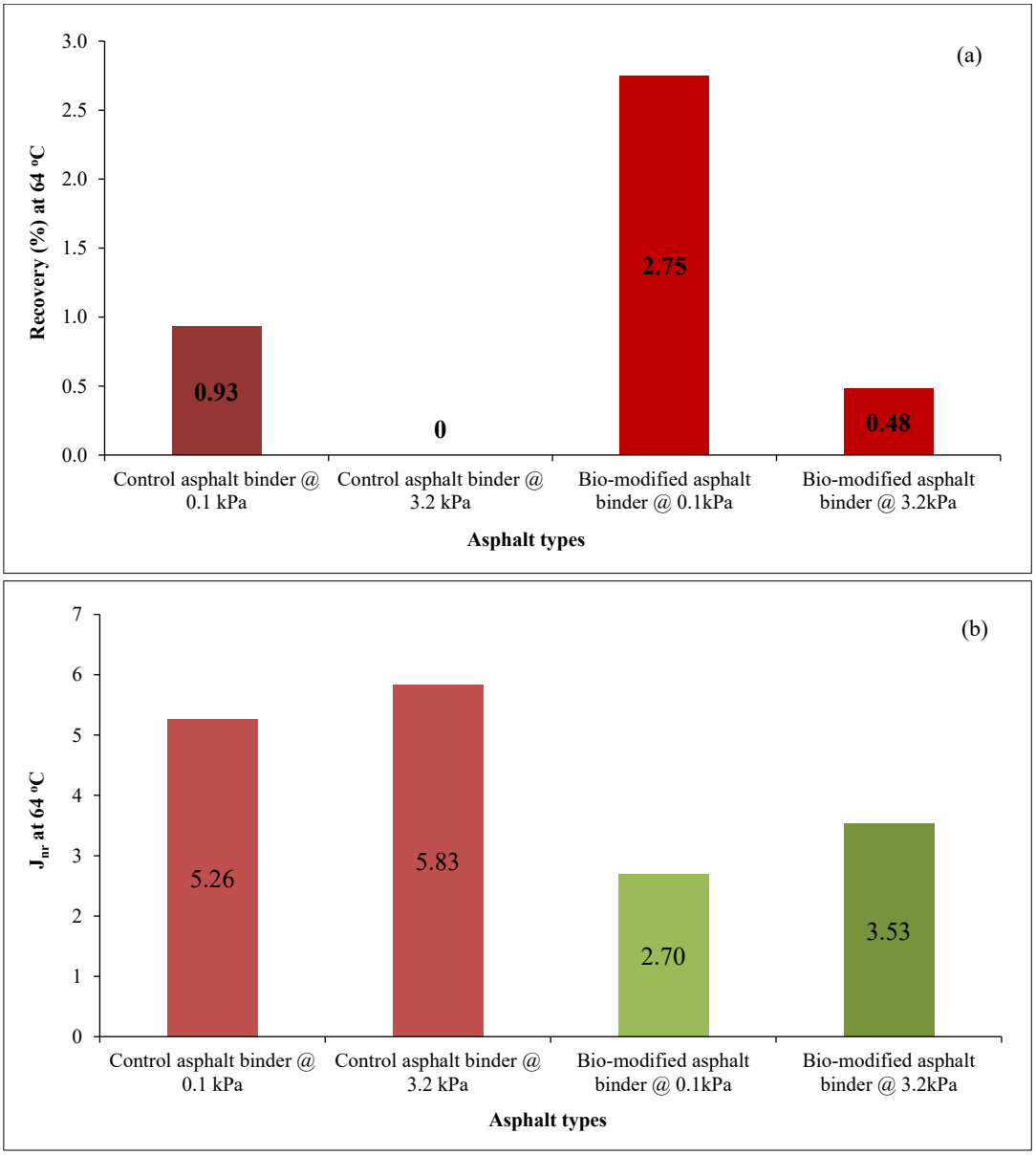

Figure 13. MSCR evaluation (a) percentage recovery and (b) J_{nr} (1/kPa) for control and bio-modified asphalt binders

3.10.2. Linear Amplitude Sweep

The LAS test was performed at 25°C to evaluate the fatigue performance of both the control asphalt binder and the bio-modified asphalt binder. As illustrated in Figure 14, the effective stress initially rises with increasing effective strain, reaches a peak at 8% strain, and subsequently declines gradually until it approaches zero. The bio-modified asphalt binder exhibits higher maximum shear stress at lower shear strain levels relative to the control asphalt binder. This behavior indicates increased stiffness relative to the control asphalt binder [63].

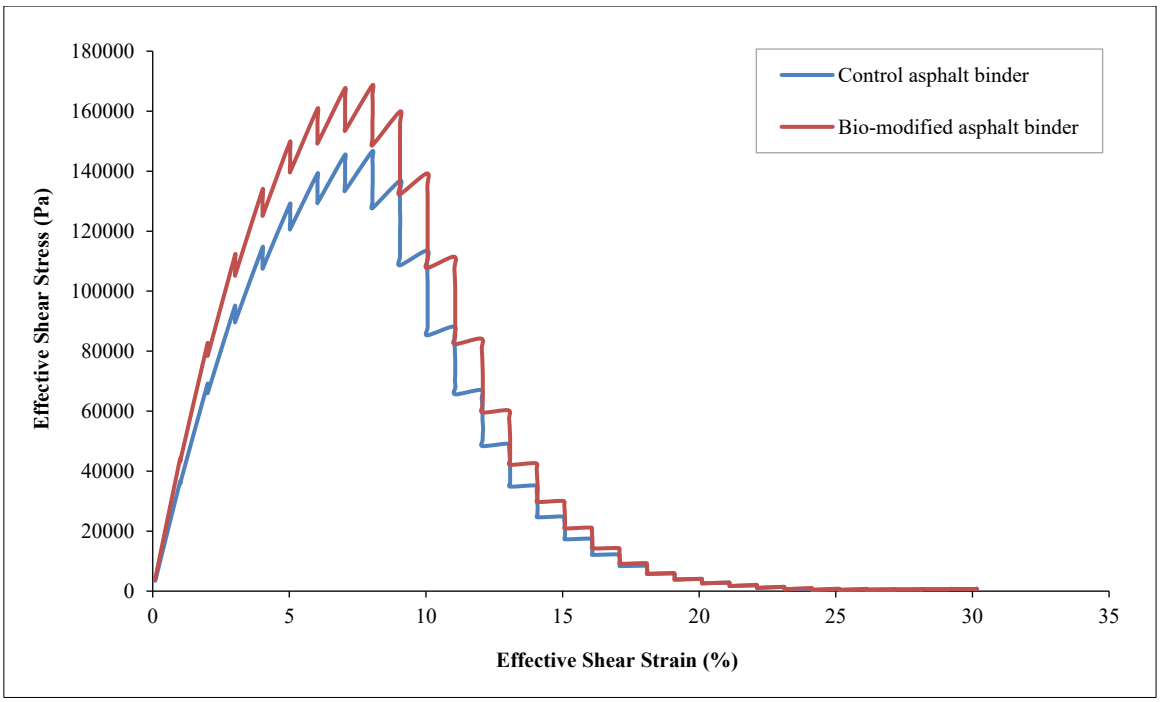

Figure 14. Stress-strain curve for control and bio-modified asphalt binders

The integrity parameter's correlation with damage intensity provides insight into the viscoelastic continuum damage mechanisms in asphalt binder [63]. Figure 15 clearly indicates that the damage intensity of the bio-modified asphalt binder is lower compared to the control binder**.** The stiffness induced by bio-asphalt mostly diminishes the ability to withstand fatigue performance.

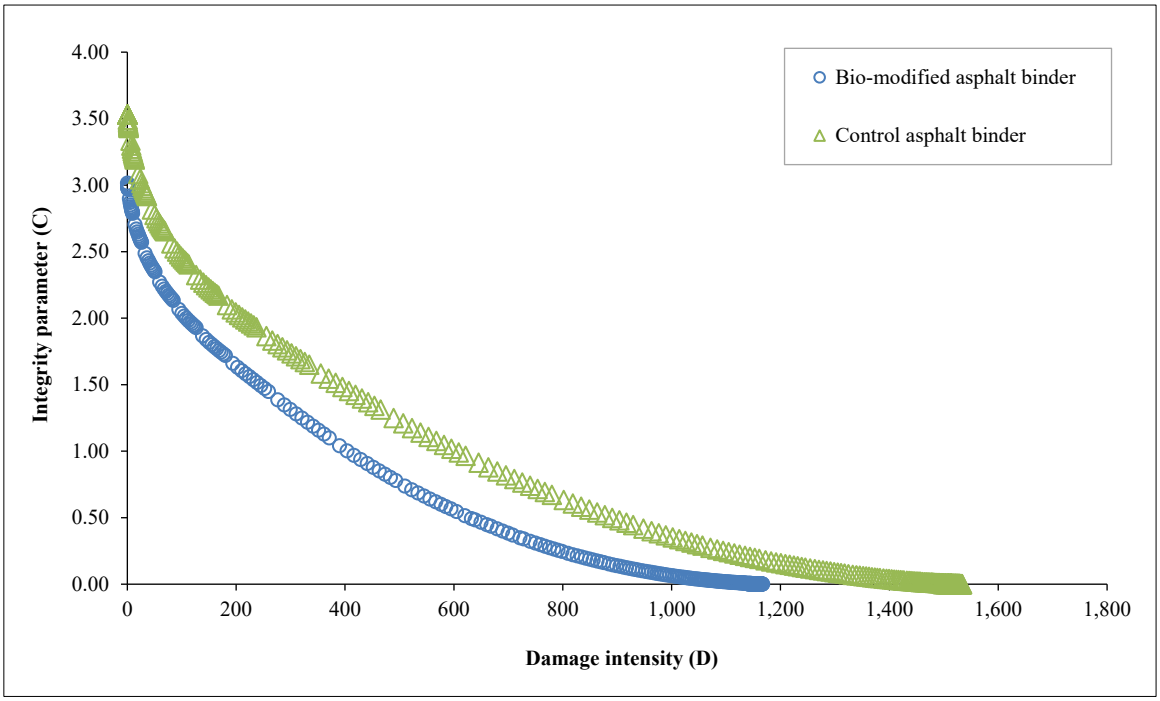

Figure 15. Viscoelastic continuum damage curve for control and bio-modified asphalt binders

Figure 16 illustrates the fatigue life (Nf) of different types of asphalt binders under two strain levels, i.e., 2.5% and 5 %. At an applied strain of 2.5%, the fatigue life of the bio-modified asphalt binder is reduced to 35.13% with respect to the control asphalt binder, and at a 5% strain level, the fatigue life drops to 18.32% in relation to the control asphalt binder. These findings indicate a reduction in the fatigue life of a bio-modified asphalt binder, signifying inferior performance compared to a control asphalt binder. This diminished performance is likely due to the increased stiffness imparted by the bio-asphalt, which reduces the binder's ability to resist fatigue cracking.

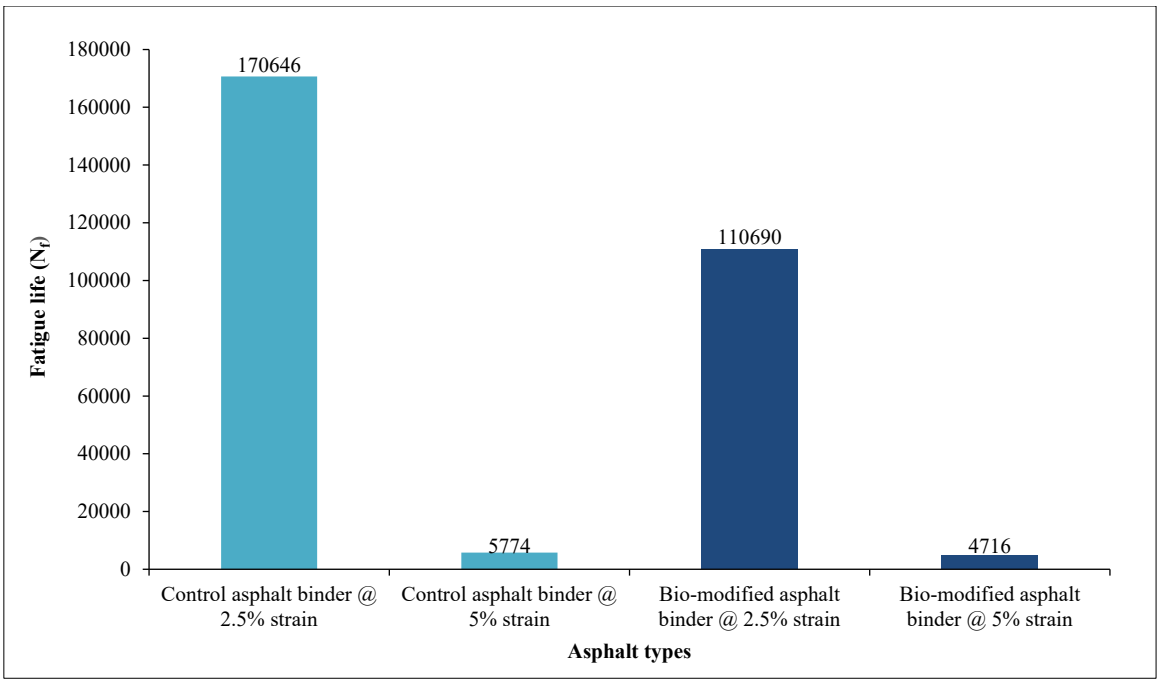

Figure 16. Fatigue life of the control and bio-modified asphalt binder

3.11. Mechanical Properties for Control Asphalt Mixture and Bio-Modified Asphalt Mixture

Three sets of control and bio-modified asphalt mixture samples were tested to evaluate various performance characteristics, including Marshall stability, retained stability, tensile strength ratio, resilient modulus, indirect tensile fatigue, and resistance to permanent deformation. The statistical parameters—mean, standard deviation, and coefficient of variation—for these tests are summarized in Table 10, while Table 11 outlines the Marshall properties of both types of mixtures. As illustrated in Figure 17, the Marshall stability of the bio-modified asphalt mixture exhibits a significant improvement, reaching 15.8 kN compared to 12.95 kN for the control mixture. This enhancement is primarily attributed to the inclusion of BA, which incorporates WCO and LDPE. LDPE, classified as a plastomer, contributes to the initial stiffness and strength of the binder, thereby increasing the mixture's ability to withstand applied load and making it more resistant to deformation under traffic loads [61]. In contrast, Figure 18 illustrates a decrease in the flow value from 3.2 mm (control asphalt mixture) to 2.9 mm (bio-modified asphalt mixture), representing a 9.38% reduction. Despite this decline, both values fall within the acceptable range of 2–4 mm, indicating that neither mixture exhibits excessive plastic deformation. The Marshall quotient, shown in Figure 19, is higher for the bio-modified mixture at 5.5, compared to 4.04 for the control mixture. This increase suggests improved resistance to rutting in the bio-modified mixture. Additionally, the retained stability rose from 86.62% (control asphalt mixture) to 94.19% (bio-modified asphalt mixture), as illustrated in Figure 20, further confirming improved moisture resistance.

Moreover, the TSR of the bio-modified asphalt mixture is 96.23%, higher than the control's 93.88%, as shown in Figure 21. The increase in TSR is due to the reinforcing effect of LDPE, which enhances the tensile properties of the binder, contributing to greater durability under moisture-induced stress. Resilient modulus testing at 25°C and 35°C shows that the bio-modified asphalt mixture outperforms the control asphalt mixture. At 25°C, the resilient modulus for the control asphalt mixture is 4683 MPa, compared to 4998 MPa for the bio-modified asphalt mixture. At 35°C, the values are 1678 MPa and 1850 MPa, respectively (Figure 22). These results indicate that the bio-modified asphalt mixture has superior resistance to deformation. However, reduction in fatigue performance is observed. As presented in Table 10, the control asphalt mixture achieves 8252 loading cycles to failure at a tensile strain of 26.5 με, while the bio-modified asphalt mixture fails at 2592 cycles under a slightly higher strain of 28.5 με. This reduced fatigue life is attributed to the use of LDPE, which, while enhancing stiffness, possesses limited strain tolerance, a common characteristic of plastomeric polymers [30]. Eventually, dynamic creep testing (Figure 23) reveals that the permanent deformation for the control asphalt mixture is 0.77 mm, whereas the bio-modified asphalt mixture records a lower value of 0.65 mm. The decreased rut depth in the bio-modified asphalt mixture sample is indicative of an enhanced ability to resist rutting. This improvement is linked to the elastic nature of the BA, particularly the presence of LDPE, which increases binder stiffness and contributes to better performance under sustained loading.

Table 10. Statistical summary of mechanical properties for control asphalt mixture and bio-modified asphalt mixture

Marshall stability (kN)		
Mix Type	**Control asphalt mixture**	**Bio-modified asphalt mixture**
Mean	12.95	15.8
Standard deviation	0.97	0.53
Coefficient of Variation (%)	0.0749	0.033
Marshall Flow (mm)		
Mix Type	**Control asphalt mixture**	**Bio-modified asphalt mixture**
Mean	3.20	2.9
Standard deviation	0.10	0.40
Coefficient of Variation (%)	0.0313	0.1379
Marshall Quotient		
Mix Type	**Control asphalt mixture**	**Bio-modified asphalt mixture**
Mean	**4.04**	**5.50**
Standard deviation	0.18	0.79
Coefficient of Variation (%)	0.0445	0.1434
Retained stability		
Mix Type	**Control asphalt mixture**	**Bio-modified asphalt mixture**
Mean	86.62	94.19
Standard deviation	0.11	0.76
Coefficient of Variation (%)	0.0012	0.0080
Tensile strength ratio (%)		
Mix Type	**Control asphalt mixture**	**Bio-modified asphalt mixture**
Mean	93.23	96.88
Standard deviation	0.24	0.67
Coefficient of Variation (%)	0.0026	0.0069
Resilient Modulus (MPa) at 25 ^{o}C		
Mix Type	**Control asphalt mixture**	**Control asphalt mixture**
Mean	4683	4998
Standard deviation	11	7
Coefficient of Variation (%)	0.0023	0.0014
Resilient Modulus (MPa) at 35 ^{o}C		
Mix Type	**Bio-modified asphalt mixture**	**Bio-modified asphalt mixture**
Mean	1678	1850
Standard deviation	9.5	5
Coefficient of Variation (%)	0.0057	0.0027

	Number cycles to failure (N_f)		**Tensile strain (με)**	
Mix Type	**Control asphalt mixture**	**Bio-modified asphalt mixture**	**Control asphalt mixture**	**Bio-modified asphalt mixture**
Mean	8252	2592	28.30	26.87
Standard deviation	100	94	1.015	0.351
Coefficient of Variation (%)	0.012	0.036	0.036	0.013

Permanent deformation @ 3600 cycles, mm		
Mix Type	**Control asphalt mixture**	**Bio-modified asphalt mixture**
Mean	0.77	0.65
Standard deviation	0.03	0.02
Coefficient of Variation (%)	0.039	0.031

Table 11. Marshall properties for control asphalt mixture and bio-modified asphalt mixture

Marshall properties	**Control asphalt mixture**	**Bio-modified asphalt mixture**	**Specification [49]**
Bulk density (g/cc)	2.35	2.32	-
Theoretical specific gravity (g/cc)	2.45	2.42	-
Vv (%)	4.4	4.2	3-5
VMA (%)	17.20	16.88	13 min
VFA (%)	74.42	74.82	65-75
Stability value (kN)	1295	1580	9
Flow value (mm)	3.2	2.9	2-4

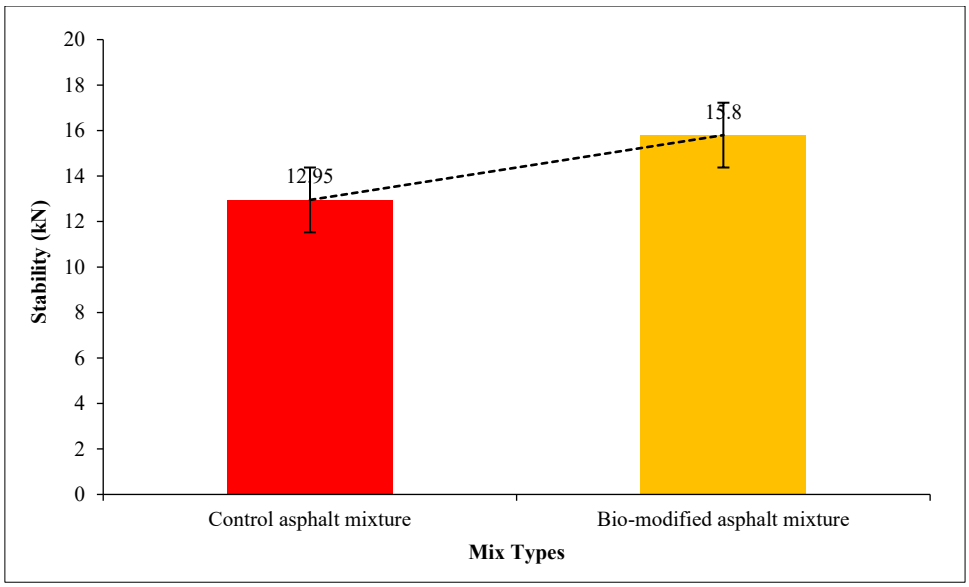

Figure 17. Marshall stability test results

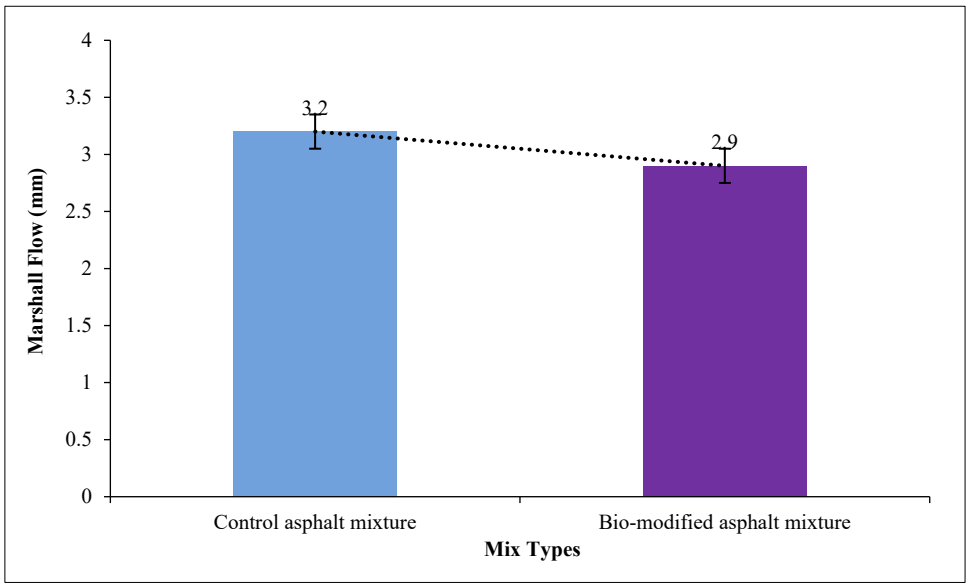

Figure 18. Marshall flow test results

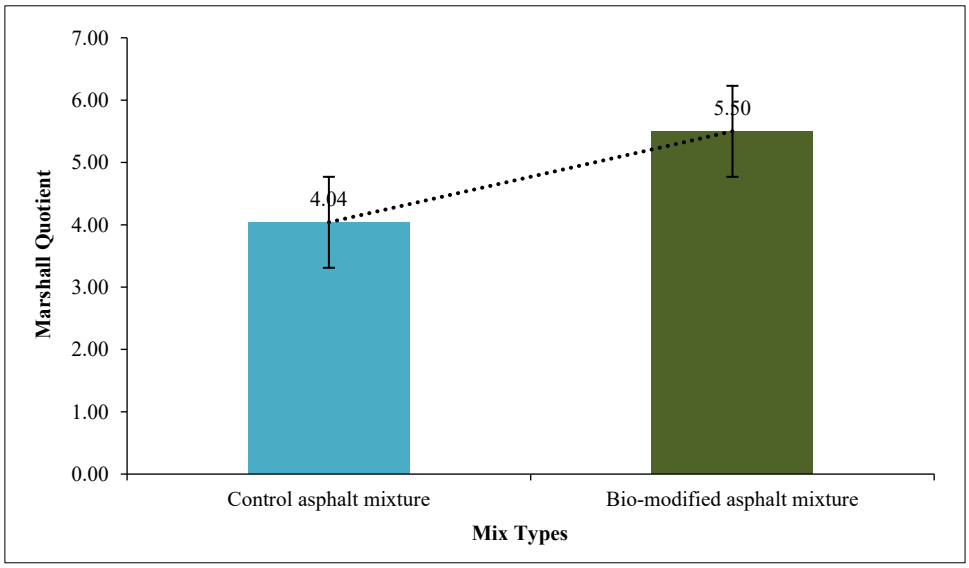

Figure 19. Marshall quotient test results

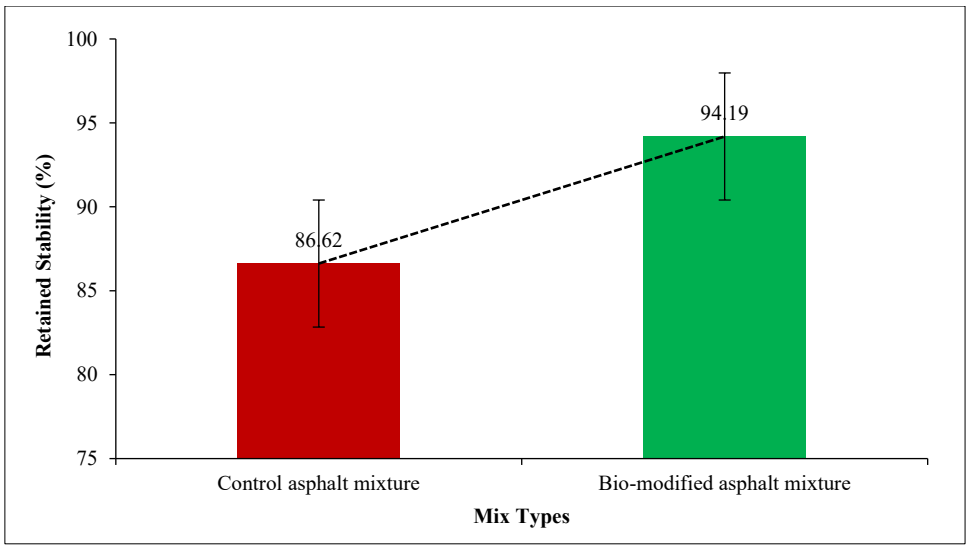

Figure 20. Retained stability test results

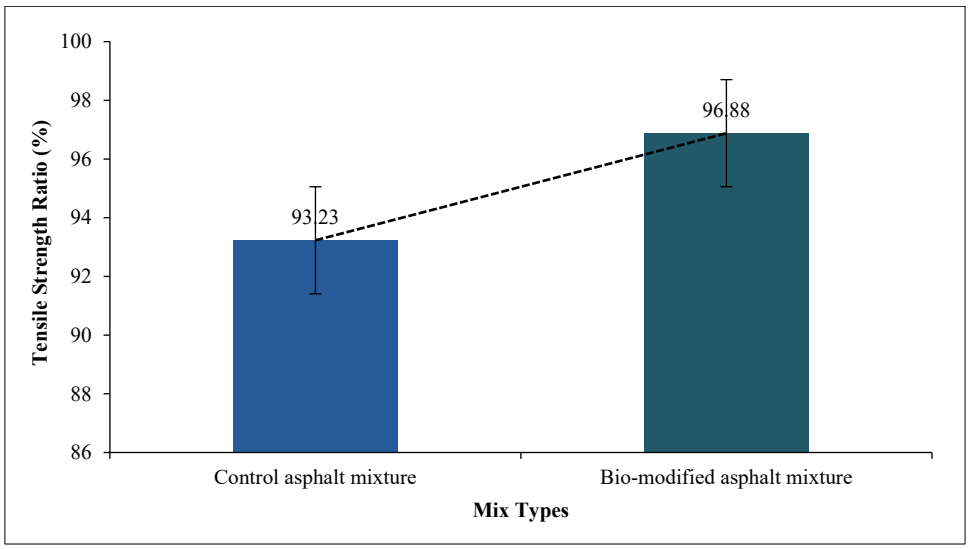

Figure 21. Tensile strength ratio test results

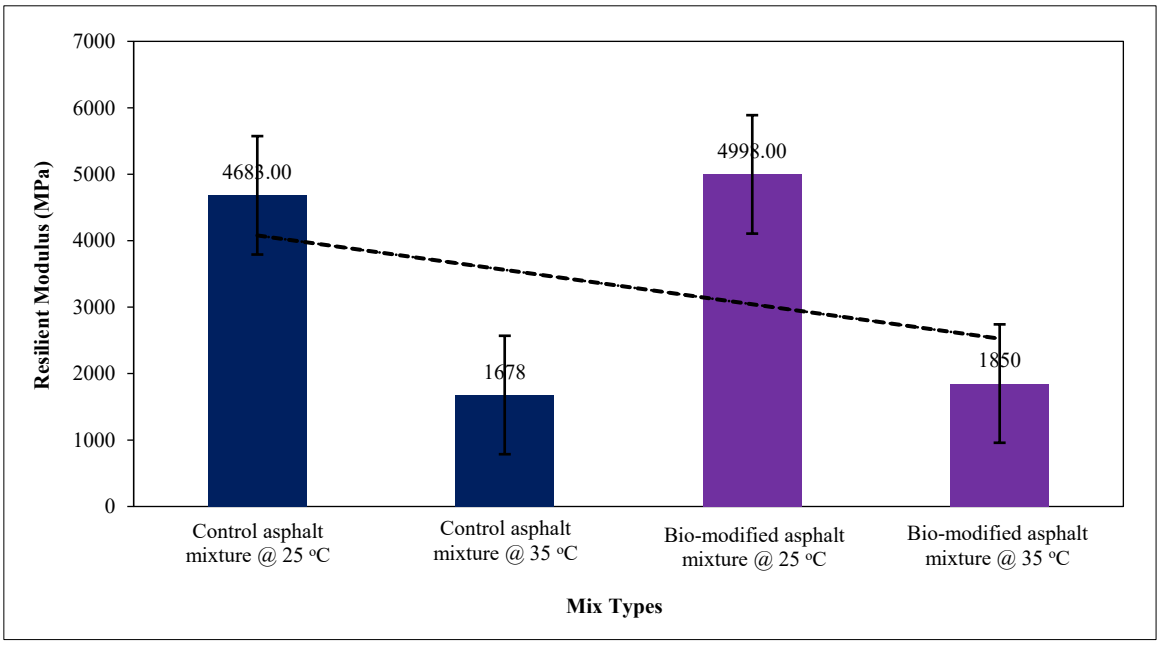

Figure 22. Resilient modulus test results

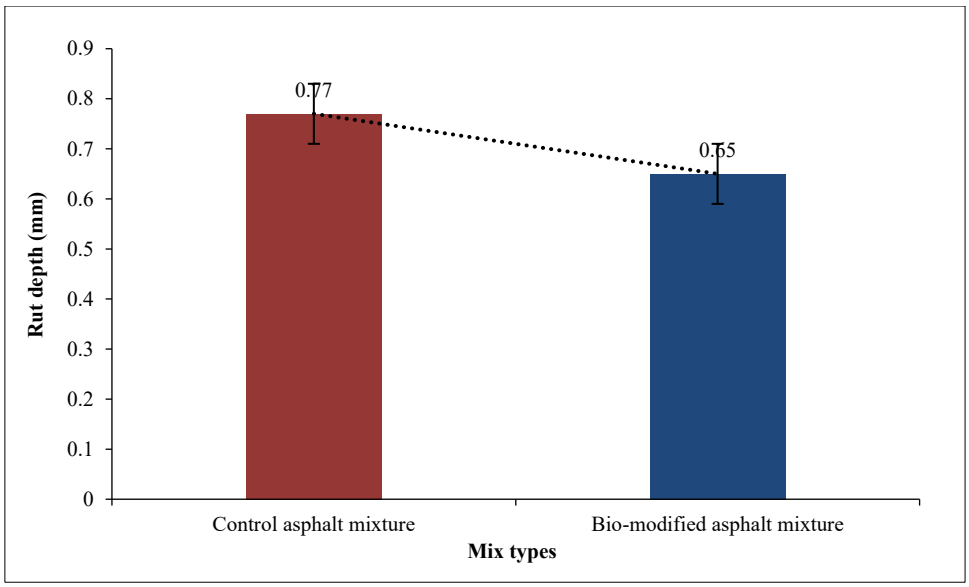

Figure 23. Dynamic creep test results

3.12. Cost Comparison of Control and Bio-Modified Asphalt Mixtures

The cost analysis involves calculating the capital expenditure required to construct a 1 km stretch of road using both conventional asphalt and bio-modified asphalt layers. Specifically, the analysis compares the total cost of laying 1 km of road with a traditional hot mix asphalt mixture against the cost of laying the same length using a bio-modified asphalt mixture. The current market price for conventional asphalt binder is approximately $533.20 per ton, whereas the cost for bio-asphalt is significantly lower, at around $118 per ton. Table 12 presents a detailed breakdown of the cost comparison between the two mixtures. The total cost for laying a 1 km stretch using bio-modified asphalt is estimated at $21,355.58, while the same road segment constructed with conventional asphalt amounts to approximately $22,100.95. This results in a cost savings of around $745.37 when opting for the bio-modified asphalt mixture. The findings clearly indicate that the use of bio-modified asphalt not only reduces construction costs but also offers a distinct economic advantage over conventional asphalt binder. This reduction in capital expenditure highlights the greater economic feasibility of bio-modified asphalt mixtures and offers a more appealing and cost-effective solution for road construction, enhancing sustainability.

Table 12. Cost Analysis for Control Asphalt Mixture and Bio-Modified Asphalt Mixture

	Optimum binder content in the mixture	Quantity of binder (ton)	Quantity of aggregates (ton)	Total cost of asphalt binder @ 533.20 $	Total cost of aggregates @ 8.29 $	Labor and transportation cost ($)	Total cost for 1km road stretch ($)
Control Asphalt Mixture	5.5%	24.23	263.15	12919.44	2181.51	7000	22100.95
	Optimum binder content in the mixture	**Quantity of binder (ton)**	**Quantity of aggregates (ton)**	**Total cost of bio-modified asphalt binder @509.63 $**	**Total cost of aggregates @ 8.29 $**	**Labor and transportation cost ($)**	**Total cost for 1km road stretch ($)**
Bio-Modified Asphalt Mixture	5.5%	23.93	260.57	12195.45	2160.13	7000	21355.58

4. Conclusions

This research focused on optimizing the blending conditions for bio-modified asphalt binders through RSM. The optimal BA content derived from RSM was then used to assess the rheological and mechanical performance of the modified binder and bio-modified asphalt mixture. The findings highlight the potential to reduce dependence on petroleum-based asphalt binders by incorporating BA.

- The developed prediction models demonstrates reliability and adequateness, as confirmed through ANOVA analysis, diagnostic plots, along with leverage and Cook's distance plots.
- The 3D and contour plots indicate that blending parameters significantly affect both penetration and softening point value, with a lower penetration value and a higher softening point leading to better performance under elevated temperature.
- The storage stability of all bio-modified asphalt binders demonstrated no phase separation, indicating the desirable compatibility of the modified binders. Additionally, a decrease in ductility values was observed with increasing BA content, suggesting a potential effect on the binder's low-temperature performance due to increased stiffness.

- By employing multi-objective optimization, the optimal values for the blending temperature, speed, and time for the bio-modified asphalt binder were determined to be 130 °C, 1000 rpm, and 42.37 min, respectively. The percentage error for each response was below 5% based on the experimental validation of the optimized blending conditions; thus, these conditions are deemed appropriate for the production of bio-modified asphalt binder.
- The rheological analysis revealed that the bio-modified asphalt binder demonstrated a higher percentage of recovery (%) and a lower non-recoverable compliance (J_{nr}) value compared to the control binder at 64°C, indicating enhanced elastic response and rutting resistance. However, at 25°C, the fatigue life (N_f) of the bio-modified binder was found to be lower than that of the control binder, which is attributed to the increased stiffness introduced by the bio-asphalt.
- The mechanical performance assessment revealed that the bio-modified asphalt mixture demonstrated enhanced Marshall stability, tensile strength ratio, resilient modulus, and resistance to permanent deformation. Nevertheless, its fatigue life was reduced as a result of the stiffening effect introduced by the bio-asphalt. The study identified an optimal dosage of bio-asphalt as an effective modifier for asphalt binders, particularly suitable for tropical climate conditions.
- From an economic standpoint, bio-modified asphalt layers offer enhanced economic feasibility, making them a more cost-effective alternative to conventional asphalt layers.

4.1. Recommendations

This investigation focuses on optimizing blending conditions for bio-modified asphalt binder and evaluating rheological and mechanical performance for optimal bio-asphalt content. However, further research is needed to explore the low-temperature performance of bio-modified asphalt binder.

5. Declarations

5.1. Author Contributions

Conceptualization, V.K.T.H., M.M., and M.S.; methodology, V.K.T.H. and M.M.; software, V.K.T.H.; validation, V.K.T.H., M.M., and M.S.; formal analysis, V.K.T.H.; investigation, V.K.T.H.; resources, V.K.T.H.; data curation, V.K.T.H.; writing—original draft preparation, V.K.T.H.; writing—review and editing, M.M. and M.S.; visualization, V.K.T.H.; supervision, M.M.; project administration, M.M.; funding acquisition, M.M. All authors have read and agreed to the published version of the manuscript.

5.2. Data Availability Statement

The data included in this study can be obtained from the corresponding author upon request.

5.3. Funding

The authors received no financial support for the research, authorship, and/or publication of this article.

5.4. Conflicts of Interest

The authors declare no conflict of interest.

6. References

[1] Yang, S. H., & Suciptan, T. (2016). Rheological behavior of Japanese cedar-based biobinder as partial replacement for bituminous binder. Construction and Building Materials, 114, 127–133. doi:10.1016/j.conbuildmat.2016.03.100.

[2] Alberta Innovates. (2021). Asphalt Binder Market Assessment. ADI Analytics, Houston, United States.

[3] Wen, H., Bhusal, S., & Wen, B. (2013). Laboratory Evaluation of Waste Cooking Oil-Based Bioasphalt as an Alternative Binder for Hot Mix Asphalt. Journal of Materials in Civil Engineering, 25(10), 1432–1437. doi:10.1061/(asce)mt.1943-5533.0000713.

[4] Gao, J., Guo, G., Wang, H., Jin, D., Bi, Y., & Jelagin, D. (2025). Research progress of bio-asphalt towards green pavement development: Preparation, properties, and mechanism. Fuel, 381. doi:10.1016/j.fuel.2024.133409.

[5] Bhavinlal, K., & Venudharan, V. (2024). Exploring production and performance of popular bio-oil modified asphalts: a state-of-the-art research review. Innovative Infrastructure Solutions, 9(10), 403. doi:10.1007/s41062-024-01716-x.

[6] Aziz, M. M. A., Rahman, M. T., Hainin, M. R., & Bakar, W. A. W. A. (2015). An overview on alternative binders for flexible pavement. Construction and Building Materials, 84, 315–319. doi:10.1016/j.conbuildmat.2015.03.068.

[7] Kantatham, K., Hoy, M., Sansri, S., Horpibulsuk, S., Suddeepong, A., Buritatum, A., … Phunpeng, V. (2024). Natural Rubber Latex-Modified Concrete with Bottom Ash for Sustainable Rigid Pavements. Civil Engineering Journal, 10(8), 2485–2501. doi:10.28991/CEJ-2024-010-08-05.

[8] Ju, Z., Ge, D., Lv, S., Jin, D., Xue, Y., Xian, J., & Zhang, W. (2024). Performance evaluation of bio-oil and high rubber content modified asphalt: More effective waste utilization. Case Studies in Construction Materials, 21. doi:10.1016/j.cscm.2024.e03828.

[9] Gao, J., Wang, H., You, Z., & Mohd Hasan, M. R. (2018). Research on properties of bio-asphalt binders based on time and frequency sweep test. Construction and Building Materials, 160, 786–793. doi:10.1016/j.conbuildmat.2018.01.048.

[10] Sun, D., Sun, G., Du, Y., Zhu, X., Lu, T., Pang, Q., Shi, S., & Dai, Z. (2017). Evaluation of optimized bio-asphalt containing high content waste cooking oil residues. Fuel, 202, 529–540. doi:10.1016/j.fuel.2017.04.069.

[11] Cavalli, M. C., Wu, W., & Poulikakos, L. (2024). Bio-based rejuvenators in asphalt pavements: A comprehensive review and analytical study. Journal of Road Engineering, 4(3), 282–291. doi:10.1016/j.jreng.2024.04.007.

[12] Al-Sabaeei, A. M., Napiah, M. B., Sutanto, M. H., Alaloul, W. S., & Usman, A. (2020). A systematic review of bio-asphalt for flexible pavement applications: Coherent taxonomy, motivations, challenges and future directions. Journal of Cleaner Production, 249. doi:10.1016/j.jclepro.2019.119357.

[13] Al-Sabaeei, A. M., Napiah, M. B., Sutanto, M. H., Alaloul, W. S., Yusoff, N. I. M., Khairuddin, F. H., & Memon, A. M. (2022). Evaluation of the high-temperature rheological performance of tire pyrolysis oil-modified bio-asphalt. International Journal of Pavement Engineering, 23(11), 4007–4022. doi:10.1080/10298436.2021.1931200.

[14] Chen, X., Li, Y., Cheng, P., Wang, H., & Nian, T. (2025). Green utilization of corn straw: Prediction of bio-oil liquefaction yield and application of bio-oil in asphalt. Industrial Crops and Products, 224, 120304. doi:10.1016/j.indcrop.2024.120304.

[15] Li, P., Yue, L., Ding, Z., Jiang, X., Li, H., An, L., & Tian, C. (2025). Review on composition properties, functionalization of bio-oil and its rejuvenation behavior and mechanism on aged asphalt. Journal of Road Engineering, 5(1), 21–34. doi:10.1016/j.jreng.2024.07.002.

[16] Liu, C., Liao, X., Fan, G., Yang, Z., Qin, X., Chen, J., & Lv, S. (2025). Utilization of bio-oil for separation of aged asphalt from reclaimed asphalt pavement: Mechanistic and experimental insights. Construction and Building Materials, 471. doi:10.1016/j.conbuildmat.2025.140743.

[17] Salimon, J., Salih, N., & Yousif, E. (2010). Biolubricants: Raw materials, chemical modifications and environmental benefits. European Journal of Lipid Science and Technology, 112(5), 519–530. doi:10.1002/ejlt.200900205.

[18] Joshi, J. R., Bhanderi, K. K., & Patel, J. V. (2023). Waste cooking oil as a promising source for bio lubricants- A review. Journal of the Indian Chemical Society, 100(1), 100820. doi:10.1016/j.jics.2022.100820.

[19] De Feo, G., Ferrara, C., Giordano, L., & Ossèo, L. S. (2023). Assessment of Three Recycling Pathways for Waste Cooking Oil as Feedstock in the Production of Biodiesel, Biolubricant, and Biosurfactant: A Multi-Criteria Decision Analysis Approach. Recycling, 8(4), 64. doi:10.3390/recycling8040064.

[20] Lin, C. S. K., Pfaltzgraff, L. A., Herrero-Davila, L., Mubofu, E. B., Abderrahim, S., Clark, J. H., Koutinas, A. A., Kopsahelis, N., Stamatelatou, K., Dickson, F., Thankappan, S., Mohamed, Z., Brocklesby, R., & Luque, R. (2013). Food waste as a valuable resource for the production of chemicals, materials and fuels. Current situation and global perspective. Energy and Environmental Science, 6(2), 426–464. doi:10.1039/c2ee23440h.

[21] van Grinsven, A., Toorn, E. van den, Veen, R. van der, & Kampman, B. (2020). Used Cooking Oil (UCO) as biofuel feedstock in the EU. CE Delft Committed to the Environment, 1–64. doi:10.13140/RG.2.2.18446.02885.

[22] Xu, N., Wang, H., Wang, H., Kazemi, M., & Fini, E. (2023). Research progress on resource utilization of waste cooking oil in asphalt materials: A state-of-the-art review. Journal of Cleaner Production, 385. doi:10.1016/j.jclepro.2022.135427.

[23] Elahi, Z., Jakarni, F. M., Muniandy, R., Hassim, S., Ab Razak, M. S., Ansari, A. H., & Ben Zair, M. M. (2021). Waste cooking oil as a sustainable bio modifier for asphalt modification: A review. Sustainability (Switzerland), 13(20), 11506. doi:10.3390/su132011506.

[24] Saboo, N., Sukhija, M., & Singh, G. (2021). Effect of Nanoclay on Physical and Rheological Properties of Waste Cooking Oil–Modified Asphalt Binder. Journal of Materials in Civil Engineering, 33(3). doi:10.1061/(asce)mt.1943-5533.0003598.

[25] Wang, C., Xue, L., Xie, W., You, Z., & Yang, X. (2018). Laboratory investigation on chemical and rheological properties of bio-asphalt binders incorporating waste cooking oil. Construction and Building Materials, 167, 348–358. doi:10.1016/j.conbuildmat.2018.02.038.

[26] Lee, S. Y., Kwak, D. Y., & Le, T. H. M. (2023). Laboratory evaluation on the aging susceptibility of reclaimed asphalt bitumen containing low-viscosity binder and cooking oil waste. Results in Engineering, 19. doi:10.1016/j.rineng.2023.101260.

[27] Jain, S., Shakyawar, P., Singh, S., & Chandrappa, A. K. (2025). The investigation of rheological properties of rejuvenated asphalt binder with waste cooking oil as rejuvenator. International Journal of Transportation Science and Technology, 18, 305–314. doi:10.1016/j.ijtst.2024.07.009.

[28] Portugal, A. C. X., Lucena, L. C. de F. L., Lucena, A. E. de F. L., Costa, D. B., & Lima, K. A. de. (2017). Rheological properties of asphalt binders prepared with maize oil. Construction and Building Materials, 152, 1015–1026. doi:10.1016/j.conbuildmat.2017.07.077.

[29] Ruikun, D., Huifang, Y., Mengzhen, Z., & Wang, H. (2022). Preparation of Asphalt Modifier Made of Waste Tire Crumb Rubber and Waste Cooking Oil. Journal of Materials in Civil Engineering, 34(8), 04022175. doi:10.1061/(asce)mt.1943-5533.0004323.

[30] Nizamuddin, S., Jamal, M., Gravina, R., & Giustozzi, F. (2020). Recycled plastic as bitumen modifier: The role of recycled linear low-density polyethylene in the modification of physical, chemical and rheological properties of bitumen. Journal of Cleaner Production, 266. doi:10.1016/j.jclepro.2020.121988.

[31] Phadke, G., & Rawtani, D. (2023). Bioplastics as polymeric building blocks: Paving the way for greener and cleaner environment. European Polymer Journal, 199. doi:10.1016/j.eurpolymj.2023.112453.

[32] Yu, X., Burnham, N. A., & Tao, M. (2015). Surface microstructure of bitumen characterized by atomic force microscopy. Advances in Colloid and Interface Science, 218, 17–33. doi:10.1016/j.cis.2015.01.003.

[33] Punith, V. S., & Veeraragavan, A. (2011). Behavior of Reclaimed Polyethylene Modified Asphalt Cement for Paving Purposes. Journal of Materials in Civil Engineering, 23(6), 833–845. doi:10.1061/(asce)mt.1943-5533.0000235.

[34] Abdy, C., Zhang, Y., Wang, J., Yang, Y., Artamendi, I., & Allen, B. (2022). Pyrolysis of polyolefin plastic waste and potential applications in asphalt road construction: A technical review. Resources, Conservation and Recycling, 180. doi:10.1016/j.resconrec.2022.106213.

[35] Khedaywi, T., Haddad, M., & Bataineh, H. (2023). Effect of waste plastic polyethylene terephthalate on properties of asphalt cement. Innovative Infrastructure Solutions, 8(9), 232. doi:10.1007/s41062-023-01208-4.

[36] Bensaada, A., Soudani, K., & Haddadi, S. (2021). Effects of short-term aging on the physical and rheological properties of plastic waste-modified bitumen. Innovative Infrastructure Solutions, 6(3), 135. doi:10.1007/s41062-021-00471-7.

[37] Ghani, U., Zamin, B., Tariq Bashir, M., Ahmad, M., Sabri, M. M. S., & Keawsawasvong, S. (2022). Comprehensive Study on the Performance of Waste HDPE and LDPE Modified Asphalt Binders for Construction of Asphalt Pavements Application. Polymers, 14(17), 3673. doi:10.3390/polym14173673.

[38] Singh, A., & Gupta, A. (2024). Mechanical and economical feasibility of LDPE Waste-modified asphalt mixtures: pathway to sustainable road construction. Scientific Reports, 14(1), 25311. doi:10.1038/s41598-024-75196-5.

[39] Abdullah, M. E., Ahmad, N. A., Jaya, R. P., Hassan, N. A., Yaacob, H., & Hainin, M. R. (2017). Effects of Waste Plastic on the Physical and Rheological Properties of Bitumen. IOP Conference Series: Materials Science and Engineering, 204(1), 012016. doi:10.1088/1757-899X/204/1/012016.

[40] Zhu, J., Lu, X., Balieu, R., & Kringos, N. (2016). Modelling and numerical simulation of phase separation in polymer modified bitumen by phase-field method. Materials and Design, 107, 322–332. doi:10.1016/j.matdes.2016.06.041.

[41] Memon, A. M., Hartadi Sutanto, M., Napiah, M., Khan, M. I., & Rafiq, W. (2020). Modeling and optimization of mixing conditions for petroleum sludge modified bitumen using response surface methodology. Construction and Building Materials, 264. doi:10.1016/j.conbuildmat.2020.120701.

[42] Kedarisetty, S., Biligiri, K. P., & Sousa, J. B. (2016). Advanced rheological characterization of Reacted and Activated Rubber (RAR) modified asphalt binders. Construction and Building Materials, 122, 12–22. doi:10.1016/j.conbuildmat.2016.06.043.

[43] Khan, K., Johari, M. A. M., Amin, M. N., Khan, M. I., & Iqbal, M. (2023). Optimization of colloidal nano-silica based cementitious mortar composites using RSM and ANN approaches. Results in Engineering, 20. doi:10.1016/j.rineng.2023.101390.

[44] Mohammed, B. S., Khed, V. C., & Nuruddin, M. F. (2018). Rubbercrete mixture optimization using response surface methodology. Journal of Cleaner Production, 171, 1605–1621. doi:10.1016/j.jclepro.2017.10.102.

[45] Mohammed, B. S., Fang, O. C., Anwar Hossain, K. M., & Lachemi, M. (2012). Mix proportioning of concrete containing paper mill residuals using response surface methodology. Construction and Building Materials, 35, 63–68. doi:10.1016/j.conbuildmat.2012.02.050.

[46] Liu, H., Zhang, M., Jiao, Y., & Fu, L. (2018). Preparation Parameter Analysis and Optimization of Sustainable Asphalt Binder Modified by Waste Rubber and Diatomite. Advances in Materials Science and Engineering, 3063620. doi:10.1155/2018/3063620.

[47] Varun, V. K., Mayakrishnan, M., & Somasundaram, M. (2024). Evaluation of the properties of bio-asphalt derived from waste cooking oil and low-density polyethylene through the pyrolysis process. Case Studies in Construction Materials, 21, 3604. doi:10.1016/j.cscm.2024.e03604.

[48] Sasidhar, K. B., Somasundaram, M., Yesuraj, K., Hariharan, S., Antunes, E., Ekambaram, P., & Kumar Arumugam, S. (2023). Optimization and production of renewable fuels from waste cooking oil and low-density polyethylene: Evaluating fuel properties and techno-economic feasibility of diesel replacement. Energy Conversion and Management, 294. doi:10.1016/j.enconman.2023.117558.

[49] Ministry of Road Transport & Highways. (2013). Specifications for Road Bridge Works (5th Revision). Indian Road Congress, new Delhi, India.

[50] IS: 73. (2013). Indian Standard Paving bitumen—Specification (Fourth Revision). Bureau of Indian Standards, New Delhi, India.

[51] Anderson, D. A., Christensen, D. W., Bahia, H. U., Dongre, R., Sharma, M. G., Antle, C. E., & Button, J. (1994). Binder characterization and evaluation, volume 3: Physical characterization. Strategic Highway Research Program, National Research Council, Washington, United States.

[52] Yan, K., Peng, Y., & You, L. (2020). Use of tung oil as a rejuvenating agent in aged asphalt: Laboratory evaluations. Construction and Building Materials, 239. doi:10.1016/j.conbuildmat.2019.117783.

[53] Zhang, H., Wu, J., Qin, Z., & Luo, Y. (2022). The effect of bio-oil on high-temperature performance of bio-oil recycled asphalt binders. Journal of Renewable Materials, 10(4), 1025–1037. doi:10.32604/JRM.2022.017483.

[54] Su, N., Xiao, F., Wang, J., Cong, L., & Amirkhanian, S. (2018). Productions and applications of bio-asphalts – A review. Construction and Building Materials, 183, 578–591. doi:10.1016/j.conbuildmat.2018.06.118.

[55] Lai, J., Wang, H., Wang, D., Fang, F., Wang, F., & Wu, T. (2014). Ultrasonic extraction of antioxidants from Chinese sumac (Rhus typhina L.) fruit using response surface methodology and their characterization. Molecules, 19(7), 9019–9032. doi:10.3390/molecules19079019.

[56] Dehouche, N., Kaci, M., & Mouillet, V. (2016). The effects of mixing rate on morphology and physical properties of bitumen/organo-modified montmorillonite nanocomposites. Construction and Building Materials, 114, 76–86. doi:10.1016/j.conbuildmat.2016.03.151.

[57] Abdullah, M. E., Zamhari, K. A., Hainin, M. R., Oluwasola, E. A., Nur, N. I., & Hassan, N. A. (2016). High temperature characteristics of warm mix asphalt mixtures with nanoclay and chemical warm mix asphalt modified binders. Journal of Cleaner Production, 122, 326–334. doi:10.1016/j.jclepro.2016.02.033.

[58] Shirzad, S., & Zouzias, H. (2024). Enhancing the performance of wood-based bio-asphalt: strategies and innovations. Clean Technologies and Environmental Policy, 26(7), 2095–2115. doi:10.1007/s10098-024-02745-x.

[59] Obaid, H. A., Eltwati, A., Hainin, M. R., Al-Jumaili, M. A., & Enieb, M. (2024). Modeling and design optimization of the performance of stone matrix asphalt mixtures containing low-density polyethylene and waste engine oil using the response surface methodology. Construction and Building Materials, 446. doi:10.1016/j.conbuildmat.2024.138037.

[60] Akinwande, M. O., Dikko, H. G., & Samson, A. (2015). Variance Inflation Factor: As a Condition for the Inclusion of Suppressor Variable(s) in Regression Analysis. Open Journal of Statistics, 5(7), 754–767. doi:10.4236/ojs.2015.57075.

[61] Hunter, R. N. (2015). The Shell Bitumen Handbook (6th Ed.). Thomas Telford Ltd., London, United Kingdom. doi:10.1680/tsbh.58378.

[62] Khairuddin, F. H., Alamawi, M. Y., Yusoff, N. I. M., Badri, K. H., Ceylan, H., & Tawil, S. N. M. (2019). Physicochemical and thermal analyses of polyurethane modified bitumen incorporated with Cecabase and Rediset: Optimization using response surface methodology. Fuel, 254. doi:10.1016/j.fuel.2019.115662.

[63] Gao, J., Wang, H., Liu, C., Ge, D., You, Z., & Yu, M. (2020). High-temperature rheological behavior and fatigue performance of lignin modified asphalt binder. Construction and Building Materials, 230. doi:10.1016/j.conbuildmat.2019.117063.